Data analysis of permanent GPS networks in Italy and surrounding regions: application of a distributed processing approach

Enrico Serpelloni ([1]), **Giuseppe Casula** ([1]), **Alessandro Galvani** ([2]), **Marco Anzidei** ([2]) **and Paolo Baldi** ([3])

([1]) *Istituto Nazionale di Geofisica e Vulcanologia, Centro Nazionale Terremoti, Bologna, Italy*
([2]) *Istituto Nazionale di Geofisica e Vulcanologia, Centro Nazionale Terremoti, Roma, Italy*
([3]) *Dipartimento di Fisica, Università degli Studi di Bologna, Italy*

Abstract
We describe the procedures used to combine into a uniform velocity solution the observations of more than 80 continuous GPS stations operating in the central Mediterranean in the 1998-2004 time interval. We used a distributed processing approach, which makes efficient use of computer resources, while producing velocity estimates for all stations in one common reference frame, allowing for an effective merging of all observations into a self-consistent network solution. We describe the CGPS data archiving and processing procedures, and provide the main results in terms of position time-series and velocities for all stations observed for more than three years. We computed horizontal and vertical velocities accounting for the seasonal (annual and semi-annual) signals, and considering the off-sets in the coordinate time-series caused by station equipment changes. Weighted post-fit RMS of the north, east and vertical velocity components are in the range of 1.57-2.08 mm, 1.31-3.28 mm, and 3.60-7.24 mm, respectively, which are reduced by solving for seasonal signals in the velocity estimates. The annual and semi-annual signals in the height components, with amplitudes up to 4.8 mm, are much stronger than those in the horizontal components. The mean amplitudes of annual and semi-annual signals are within 0.18-0.47 mm, 0.23-0.52 mm and 0.55-1.92 mm in the north, east and vertical components, respectively.

Key words *Global Positioning System (GPS) – continuous monitoring – Central Mediterranean – time series analysis*

1. Introduction

The rapid development of modern space geodesy techniques over the last two decades provided important new data that introduced significant constraints on the active geological processes occurring in the Mediterranean area (*e.g.*, Battaglia *et al.*, 2004; D'Agostino and Selvaggi, 2004; Goes *et al.*, 2004; D'Agostino *et al.*, 2005; Serpelloni *et al.*, 2005; among others). Earlier GPS studies used either very large or sparse global networks (*e.g.*, Larson *et al.*, 1997), focusing only on the large scale tectonic aspects (*i.e.*, the motion of major tectonic plates, intra-plate rigidity), or dense but small aperture networks, focusing only on local tectonic processes, such as deformation along particular segments of fault zones (*e.g.*, Anzidei *et al.*, 1998). The difficulties in tying such a different scale networks into a common reference frame has been one of the main obstacles in un-

Mailing address: Dr. Enrico Serpelloni, Istituto Nazionale di Geofisica e Vulcanologia, Centro Nazionale Terremoti, Via Donato Creti 12, 40128 Bologna, Italy; e-mail: serpelloni@bo.ingv.it

derstanding the active tectonic processes in diffusely deforming continental plate boundaries, which are of great scientific interest for seismic hazard aspects. During the last 10 years, the rapid development of the global GPS technique, mainly under the umbrella of the International GPS Service for Geodynamics consortium (IGS; http://igscb.jpl.nasa.gov), provided more precise determination of satellite orbital parameters, through the enlargement of the GPS satellite constellation, and the improvement of the global Continuous GPS (CGPS) tracking station coverage. Moreover, the establishment of regional networks of CGPS stations (*e.g.*, EPN-EUREF, ASI, Regal, FredNet networks) increased the number of stations available to tie observations together interferometrically. This technological development significantly increased the precision of station position determinations, reducing the noise spectra of the solutions, and allowing for a better resolution of the coordinate changes detection, even in the vertical component. This is fundamental in areas characterized by low deformation rates, such as the western and central Mediterranean and the European region (McClusky *et al.*, 2003; Nocquet and Calais 2003), where an accurate estimate of crustal deformation parameters mainly requires the use of CGPS stations.

In Italy, several CGPS stations are operated and managed by different agencies, private companies and national scientific institutions (see Sansò and De Lacy, 2000, available at http://geomatica.como.polimi.it/gps/articoli/asi.pdf), but most of these stations have been built for different purposes (*i.e.*, topography, cartography, tele-communication, crustal deformation monitoring, navigation, etc.). Unfortunately, the number of sites that match the minimum requirements needed for geophysical applications (antenna/receiver features and monumentation quality), and for which raw data are freely available on the internet is actually not enough to provide an exhaustive description of the deformation pattern of such a high tectonically fragmented zone. For this reason the use of high quality non-permanent GPS data, collected over significantly long time span (at least 5 years) by means of repeated campaigns, is still fundamental to improve the spatial and temporal resolution of the

crustal deformation field in the study area (*e.g.*, Serpelloni *et al.*, 2002, 2005).

In recent years the number of CGPS stations suitable for geophysical applications has rapidly increased, particularly in the frame of INGV activities. In this prospective, we developed automatic facilities to handle the CGPS data archiving and data processing procedures. In this work we present an application of the «distributed processing» technique, used to merge most of the available CGPS networks operating in the central Mediterranean, with the goal of obtaining a single network solution, and formally no more considering the different networks separately. Moreover, the data analysis approach followed allows us to obtain velocity vectors of stations belonging to networks whose raw data are not directly processed. We describe in detail the procedures used to collect, store and process the raw data in order to combine all these information into one uniform crustal velocity field. Results can be further used for geo-kinematics purposes, and for a better understanding of the active geodynamic processes that are deforming the Earth's surface in Italy and surrounding regions. A detailed tectonics interpretation of the presented results is, however, beyond the scope of this work.

2. Continuous GPS networks in the study area

In the last ten years the number of CGPS sites operating in the Central Mediterranean region has significantly increased. Since the amount of stations belonging to the global and European networks (*i.e.*, IGS and EUREF networks) is still too small, to enlarge our analysis outside Italy we collect and process data coming from other regional CGPS networks in France and Austria. Figure 1a,b shows the distribution of the 81 CGPS stations for which we routinely download and processes raw data to produce position time-series. Table I reports some information related to these sites, which belong to the networks described in the following paragraphs.

IGS – The International GPS Service, along with a multinational membership of organizations and agencies, maintains a global network of over 350 continuously operating dual-fre-
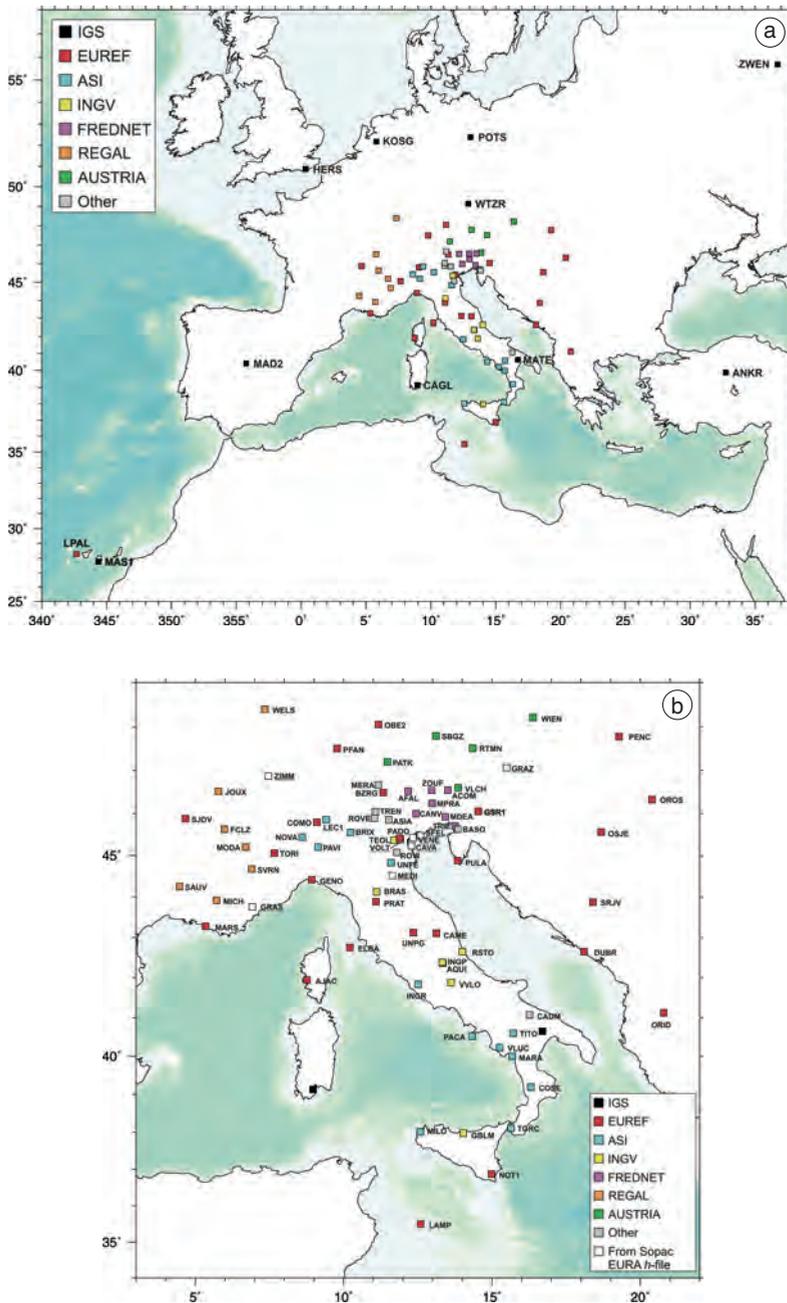
Fig. 1a,b. a) Euro-Mediterranean map showing the distribution of the CGPS stations archived, processed and discussed in this work. The names of the IGS stations used are also displayed. b) Central Mediterranean map showing the distribution and names (4 character ID code), of the CGPS stations archived, processed and discussed in this work.

Table 1. List of the continuous GPS stations archived and analyzed in this work. Columns from left to right display: station number, full name, longitude, latitude, four character ID, network to which the station formally belongs (IGS – International GPS Service network; EUREF – EUropean REFerence network; ASI – Agenzia Spaziale Italiana network; FREDNET – FRiuli REgional Deformation NETwork; INGV – Istituto Nazionale di Geofisica e Vulcanologia network; REGAL – REseau GPS permanent dans les ALpes network; AUSTRIA – Austrian GPS network; OTHER – other stations not belonging to any specific network), remote ftp archive addresses for data downloading, source for the equipment changes information (*sopac* – from SOPAC *station.info* file; *epn* – from EUREF station history file; *log* – from station log file; *rnx* – from RINEX file header), number referring to the cluster in which the station is processed (1 – southern cluster, 2 – northern cluster; 3 – mixed cluster), station monument descriptions.

No.	Station name	Long	Lat	ID	Net	FTP archive	Stinfo	SN	Monument type
1	Ankara	32.75	39.88	ANKR	IGS	ftp://lox.ucsd.edu/pub/rinex/yyyy/ddd	*sopac*	1, 2, 3	Pillar on weathered bedrock (limestone)
2	Cagliari	8.97	39.13	CAGL	IGS	ftp://lox.ucsd.edu/pub/rinex/yyyy/ddd	*sopac*	1, 2, 3	Pillar on igneous bedrock
3	Herstmonceaux	0.33	50.87	HERS	IGS	ftp://lox.ucsd.edu/pub/rinex/yyyy/ddd	*sopac*	1, 2, 3	8 m height steel mast on unconsolidated soils
4	Kootwijk	5.81	52.18	KOSG	IGS	ftp://lox.ucsd.edu/pub/rinex/yyyy/ddd	*sopac*	1, 2, 3	-
5	Madrid	−4.25	40.43	MAD2	IGS	ftp://lox.ucsd.edu/pub/rinex/yyyy/ddd	*sopac*	1, 2, 3	Brass disk on roof of building founded on unconsolidated soils (sands)
6	Mas Palomas	−15.63	27.76	MAS1	IGS	ftp://lox.ucsd.edu/pub/rinex/yyyy/ddd	*sopac*	1, 2, 3	Pillar on bedrock
7	Matera	16.70	40.65	MATE	IGS	ftp://lox.ucsd.edu/pub/rinex/yyyy/ddd	*sopac*	1, 2, 3	Pillar on roof of building founded on sedimentary bedrock
8	Potsdam	13.06	52.38	POTS	IGS	ftp://lox.ucsd.edu/pub/rinex/yyyy/ddd	*sopac*	1, 2, 3	Pillar on building founded on sediments
9	Tromso	18.94	69.66	TRO1	IGS	ftp://lox.ucsd.edu/pub/rinex/yyyy/ddd	*sopac*	1, 2, 3	5.5 m steel mast on fresh sedimentary/ metamorphic bedrock
10	Wettzell	12.88	49.14	WTZR	IGS	ftp://lox.ucsd.edu/pub/rinex/yyyy/ddd	*sopac*	1, 2, 3	Steel plate on concrete tower founded on weathered igneous bedrock
11	Zwen Astronomical	36.75	55.69	ZWEN	IGS	ftp://lox.ucsd.edu/pub/rinex/yyyy/ddd	*sopac*	1, 2, 3	Pillar on the roof of building
12	Ajaccio	8.76	41.93	AJAC	EUREF	ftp://igs.ifag.de/EUREF/obs/year/doy	*sopac*	1	Reinforced concrete pillar on igneous bedrock
13	Aquila	13.35	42.37	AQUI	EUREF	ftp://igs.ifag.de/EUREF/obs/year/doy	*sopac*	1	Pillar on sedimentary bedrock
14	Bolzano	11.34	46.49	BZRG	EUREF	ftp://igs.ifag.de/EUREF/obs/year/doy	*sopac*	2	Steel pillar on the roof of building
15	Camerino	13.12	43.11	CAME	EUREF	ftp://igs.ifag.de/EUREF/obs/year/doy	*sopac*	1	Pillar on sedimentary bedrock
16	Como	9.09	45.80	COMO	EUREF	ftp://geodaf.mt.asi.it/GEOD/GPSD/RAW/yyyy/ddd	*log*	2	Stable pillar on roof of building founded on fresh sedimentary bedrock (sand/clays)
17	Dubrovnic	18.11	42.65	DUBR	EUREF	ftp://igs.ifag.de/EUREF/obs/year/doy	*epn*	1	Steel tripod anchored to flat roof of building founded on weathered sedimentary bedrock
18	Elba	10.21	42.75	ELBA	EUREF	ftp://igs.ifag.de/EUREF/obs/year/doy	*epn*	1	Stable pillar on bedrock
19	Genova	8.92	44.42	GENO	EUREF	ftp://igs.ifag.de/EUREF/obs/year/doy	*sopac*	2	Pillar on the roof of building founded on folded sedimentary bedrock

Table I (*continued*).

No.	Station name	Long	Lat	ID	Net	FTP archive	Stinfo	SN	Monument type
20	Geoservis GS-REF1	14.54	46.05	GSR1	EUREF	ftp://igs.ifag.de/EUREF/obs/year/doy	*epn*	2	1.5 m steel mast on the top of building
21	Lampedusa	12.60	35.50	LAMP	EUREF	ftp://igs.ifag.de/EUREF/obs/year/doy	*sopac*	1	Steel mast on the roof of building
22	La Palma	–17.32	28.27	LPAL	EUREF	ftp://igs.ifag.de/EUREF/obs/year/doy	*epn*	1	Reinforced concrete pillar on the top of roof of a 3 m height building founded on bedrock
23	Marsiglia	5.35	43.28	MARS	EUREF	ftp://igs.ifag.de/EUREF/obs/year/doy	*sopac*	2	Aluminum plate on the terrace of building founded on sedimentary bedrock (clays)
24	Noto	14.99	36.87	NOT1	EUREF	ftp://lox.ucsd.edu/pub/rinex/yyyy/ddd	*sopac*	1, 2, 3	Concrete pillar founded on sedimentary bedrock
25	Oberpfaffenhofen	11.18	48.06	OBE2	EUREF	ftp://igs.ifag.de/EUREF/obs/year/doy	*sopac*	2	2.51 m height steel mast on the roof of building
26	Ohrid	20.79	41.12	ORID	EUREF	ftp://igs.ifag.de/EUREF/obs/year/doy	*sopac*	1	Concrete pillar on jointed sedimentary bedrock
27	Oroshaza	20.40	46.33	OROS	EUREF	ftp://igs.ifag.de/EUREF/obs/year/doy	*epn*	1	Forced centered marker tied on an unused chimney founded on weathered sedimentary bedrock
28	Osijec	18.68	45.56	OSJE	EUREF	ftp://igs.ifag.de/EUREF/obs/year/doy	*sopac*	1	1 m height steel mast anchored on the wall of roof on weathered sedimentary bedrock
29	Padova	11.89	45.41	PADO	EUREF	ftp://lox.ucsd.edu/pub/rinex/yyyy/ddd	*sopac*	1, 2, 3	Steel plate on the roof of building founded on sedimentary bedrock (clay/sand)
30	Penc	19.28	47.78	PENC	EUREF	ftp://lox.ucsd.edu/pub/rinex/yyyy/ddd	*sopac*	2	Concrete pillar on the roof of building founded on stable sedimentary bedrock
31	Pfaender	9.78	47.51	PFAN	EUREF	ftp://igs.ifag.de/EUREF/obs/year/doy	*sopac*	2	2 m steel mast on fresh sedimentary bedrock
32	Prato	11.09	43.88	PRAT	EUREF	ftp://geodaf.mt.asi.it/GEOD/GPSD/RAW/yyyy/ddd	*sopac*	2	Concrete pillar on roof of building founded on sedimentary (send/gravel) bedrock
33	Saint Jean des Vignes	4.67	45.88	SJDV	EUREF	ftp://igs.ifag.de/EUREF/obs/year/doy	*sopac*	2	Steel mast on top of small concrete building directly anchored into bedrock (limestone)
34	Saraievo	18.41	43.87	SRJV	EUREF	ftp://igs.ifag.de/EUREF/obs/year/doy	*sopac*	1	Steel mast on chimney of stable building
35	Torino	7.66	45.06	TORI	EUREF	ftp://igs.ifag.de/EUREF/obs/year/doy	*sopac*	1, 2, 3	Steel mast at top of wall on stable building founded on sediments
36	Perugia	12.35	43.12	UNPG	EUREF	ftp://igs.ifag.de/EUREF/obs/year/doy	*sopac*	1	Stale concrete pillar on top of roof of building founded on jointed sedimentary (fluvial) bedrock
37	Brescia	10.23	45.55	BRIX	ASI	ftp://geodaf.mt.asi.it/GEOD/GPSD/RAW/yyyy/ddd	*log*	2	Pillar on roof of building founded on sediments (sand/gravel)

Table I (*continued*).

No.	Station name	Long	Lat	ID	Net	FTP archive	Stinfo	SN	Monument type
38	Cosenza	16.31	39.20	COSE	ASI	ftp://geodaf.mt.asi.it/GEOD/GPSD/RAW/yyyy/ddd	*sopac*	3	Stable pillar on the roof of building founded on fresh metamorphic bedrock
39	ING-Roma	12.51	41.83	INGR	ASI	ftp://geodaf.mt.asi.it/GEOD/GPSD/RAW/yyyy/ddd	*log*	1	Stable pillar on roof of building founded on not fractured piroclastic bedrock
40	Lecco	9.24	45.51	LEC1	ASI	ftp://geodaf.mt.asi.it/GEOD/GPSD/RAW/yyyy/ddd	*log*	3	Stable pillar on roof of building founded on sedimentary bedrock (sand/gravel)
41	Maratea	15.69	40.00	MARA	ASI	ftp://geodaf.mt.asi.it/GEOD/GPSD/RAW/yyyy/ddd	*log*	1	Stable pillar on roof of building founded on jointed sedimentary bedrock
42	Milo (TP)	12.58	38.01	MILO	ASI	ftp://geodaf.mt.asi.it/GEOD/GPSD/RAW/yyyy/ddd	*log*	1	Stable concrete pillar founded on sedimentary bedrock
43	Novara	8.61	45.44	NOVA	ASI	ftp://geodaf.mt.asi.it/GEOD/GPSD/RAW/yyyy/ddd	*sopac*	1	-
44	Palma Campania	14.33	40.52	PACA	ASI	ftp://geodaf.mt.asi.it/GEOD/GPSD/RAW/yyyy/ddd	*log*	1	Stable iron pillar on the roof of building founded on sedimentary bedrock
45	Pavia	9.13	45.20	PAVI	ASI	ftp://geodaf.mt.asi.it/GEOD/GPSD/RAW/yyyy/ddd	*rnx*	2	-
46	Reggio Calabria	15.64	38.11	TGRC	ASI	ftp://geodaf.mt.asi.it/GEOD/GPSD/RAW/yyyy/ddd	*log*	1	Stable pillar on roof of building
47	Tito Scalo	15.72	40.60	TITO	ASI	ftp://geodaf.mt.asi.it/GEOD/GPSD/RAW/yyyy/ddd	*log*	1	Stable pillar on roof of building founded on shale
48	Ferrara	11.60	44.83	UNFE	ASI	ftp://geodaf.mt.asi.it/GEOD/GPSD/RAW/yyyy/ddd	*sopac*	2	Metallic pillar on the roof of building founded on alluvial sends
49	Vallo della Lucania	15.26	40.23	VLUC	ASI	ftp://geodaf.mt.asi.it/GEOD/GPSD/RAW/yyyy/ddd	*sopac*	1	Stable pillar on the roof of building
50	Monte Acomizza	13.52	46.55	ACOMF	FREDNET	ftp://wave.crs.inogs.it/pub/gps/rinex/yyyy/ddd	*sopac*	2	Concrete reinforced pillar founded on fresh bedrock (limestone)
51	Alpe Faloria	12.18	46.53	AFAL	FREDNET	ftp://wave.crs.inogs.it/pub/gps/rinex/yyyy/ddd	*sopac*	2	Concrete reinforced pillar founded on fresh bedrock (limestone)
52	Caneva	12.43	46.00	CANV	FREDNET	ftp://wave.crs.inogs.it/pub/gps/rinex/yyyy/ddd	*sopac*	2	Concrete reinforced pillar founded on fresh bedrock (limestone)
53	Colle di Medea	13.44	45.92	MDEA	FREDNET	ftp://wave.crs.inogs.it/pub/gps/rinex/yyyy/ddd	*sopac*	2	Concrete reinforced pillar founded on fresh bedrock (limestone)
54	Mont di Prat	12.99	46.24	MPRA	FREDNET	ftp://wave.crs.inogs.it/pub/gps/rinex/yyyy/ddd	*sopac*	2	Concrete reinforced pillar founded on fresh bedrock (limestone)
55	Trieste	13.76	45.71	TRIE	FREDNET	ftp://wave.crs.inogs.it/pub/gps/rinex/yyyy/ddd	*sopac*	2	Steel mast anchored to the wall of building

Table I (*continued*).

No.	Station name	Long	Lat	ID	Net	FTP archive	Stinfo	SN	Monument type
56	Zouf	12.58	46.33	ZOUF	FREDNET	ftp://wave.crs.inogs.it/pub/gps/rinex/yyyy/ddd	sopac	2	Concrete reinforced pillar founded on fresh bedrock (limestone)
57	Brasimone	11.11	44.12	BRAS	INGV/UNIBO	ftp://lox.ucsd.edu/pub/rinex/yyyy/ddd	sopac	1, 2, 3	Concrete block on roof of building
58	Gibilmanna	14.03	37.98	GBLM	INGV	CONV	log	1	Concrete pillar on bedrock
59	Preturo	13.32	42.38	INGP	INGV	LOCAL	log	3	Concrete pillar on bedrock
60	Roseto degli Abruzzi	14.00	42.65	RSTO	INGV	CONV	log	3	Concrete pillar founded on sediments
61	Teolo	11.70	45.37	TEOL	INGV	CONV	log	2	Concrete reinforced pillar on jointed bedrock
62	Villa Valle Longa	13.62	41.87	VVLO	INGV	CONV	log	3	Steel mast on sedimentary bedrock (limestone)
63	Chatel de Joux	5.78	46.52	JOUX	REGAL	ftp://kreiz.unice.fr/pub/Regal/serrurier/yyyy	log	2	Concrete pillar on fresh sedimentary bedrock
64	La Feclaz	5.98	45.63	FCLZ	REGAL	ftp://kreiz.unice.fr/pub/Regal/yyyy	log	2	Concrete pillar on fresh sedimentary bedrock
65	Saint Michel l'Obs.	5.72	43.92	MICH	REGAL	ftp://lareg.ensg.ign.fr/pub/rgp/yyyy/ddd	log	2	Concrete pillar on fresh sedimentary bedrock
66	Modane	6.70	45.20	MODA	REGAL	ftp://lareg.ensg.ign.fr/pub/rgp/yyyy/ddd	log	2	Antenna fixed on top of concrete platform anchored into fresh metamorphic bedrock
67	Le Sauvan	4.47	44.25	SAUV	REGAL	ftp://kreiz.unice.fr/pub/Regal/yyyy	log	2	Concrete pillar on fresh sedimentary bedrock
68	Saint Véran	6.90	44.68	SVRN	REGAL	ftp://kreiz.unice.fr/pub/Regal/yyyy	log	2	Concrete pillar on fresh bedrock
69	Welschbruch	7.35	48.40	WELS	REGAL	ftp://kreiz.unice.fr/pub/Regal/yyyy	log	2	
70	Patscherkofel	11.47	47.20	PATK	AUSTRIA	ftp://olggps.oeaw.ac.at/pub/outdata/patk	rnx	2	Concrete pillar and steel mast anchored on granite bedrock
71	Rottenmann	14.35	47.52	RTMN	AUSTRIA	ftp://olggps.oeaw.ac.at/pub/outdata/rttmn	rnx	2	Concrete pillar and steel mast on roof of building
72	Salzburg	13.12	47.80	SBGZ	AUSTRIA	ftp://igs.ifag.de/EUREF/obs/year/doy	sopac	2	Concrete pillar and steel mast anchored on sedimentary bedrock
73	Villach	13.87	46.60	VLCH	AUSTRIA	ftp://olggps.oeaw.ac.at/pub/outdata/vlch	rnx	2	-
74	Vienna	16.38	48.22	WIEN	AUSTRIA	ftp://olggps.oeaw.ac.at/pub/outdata/wien	rnx	2	Steel mast on roof of building
75	Asiago	11.53	45.85	ASIA	OTHER	CONV	rnx	2	-
76	Basovizza	13.85	45.63	BASO	OTHER	LOCAL	log	3	Concrete block on bedrock
77	Castel del Monte	16.27	41.07	CADM	OTHER	CONV	log	3	Pillar on roof of building
78	Merano	11.17	46.67	MERA	OTHER	CONV	rnx	3	-
79	Rovereto	11.04	45.89	ROVE	OTHER	CONV	rnx	3	-
80	Rovigo	11.79	45.07	ROVI	OTHER	CONV	rnx	2	-
81	Trento	11.07	46.04	TREN	OTHER	CONV	rnx	3	Steel mast on roof of building

quency GPS stations, which provides on line high-quality data in near real time. These data sets are used by the IGS to generate several data products (*i.e.*, GPS satellite ephemeredes, Earth rotation parameters, tracking station coordinates and velocities, GPS satellite and IGS tracking station clock information, Zenith tropospheric path delay estimates, global ionospheric maps, etc.), available through the Internet. The accuracies of IGS products are sufficient for the improvement and extension of the International Terrestrial Reference Frame (ITRF), the monitoring of solid Earth deformations, the monitoring of Earth rotation and variations in the fluid Earth (sea level, ice-sheets, etc.), for high precision satellite orbit determinations, ionosphere and troposphere studies. While from a constructive point of view the IGS network is largely heterogeneous, the stations have to meet some restricted requirements, both in terms of data quality and monument stability over time. We currently download and analyze the raw data coming from 11 IGS stations in the Euro-Mediterranean region (black squares in fig. 1a,b; NYA1 is outside map), chosen to constitute the subset of sites that are common to all the subnetworks analyzed and allowing for further combinations.

EUREF – The EUREF Permanent Network (EPN; http://epncb.oma.be/) represents the densification of the IGS network in Europe, and was setup in 1995. The EPN is a science-driven network of permanent GPS tracking stations whose weekly computed positions are used by EUREF to realize the European Terrestrial Reference System. The EPN is also valuable for scientific applications, such as geodynamics, sea level monitoring and weather prediction. More than 150 EPN stations, distributed over 32 European countries, provide near real time high quality GPS data, archived at local and regional data centers. EPN analysis centers routinely analyze the data from this network and deliver to the GPS community data products, including precise coordinates for all stations, satellite ephemeredes, Earth Orientation Parameters (EOP), etc. The EPN tracking stations are integrated in the successive realizations of the International Terrestrial Reference System. As for the IGS network, also the EPN stations must follow some restricted requirements

in terms of data quality and monument stability. However, most of these stations are built on roof of buildings or set up with quite poor monuments, which can reduce the tectonic significance of the detected signal. We routinely process the data coming from 25 EPN stations, which are located in and around the Italian region (see fig. 1a,b).

ASI – In 1995 the Italian Space Agency (ASI) established some permanent GPS stations to constitute the Italian GPS Fiducial network, together with some of the fundamental stations, like Matera (belonging to the IGS core sites network), active from the 1991. The ASI network (http://geodaf.mt.asi.it/html/browse.html) is constituted by 32 stations, some of them belonging to other networks (*e.g.*, IGS, EPN, INGV and Frednet). This network includes stations for which data and monument quality requirements are not as tight as for the IGS and EPN networks. ASI stations, in fact, display a large variability of monument typologies and antenna/receiver combinations, and most of them are built on roof of buildings. Standard station log-files are available on the GEODAF web site. We analyze all the RINEX data coming from the ASI network.

INGV – In 1997, the Istituto Nazionale di Geofisica e Vulcanologia (INGV), began to setup a permanent GPS network in Italy. The network has been established with the aim to detect crustal deformation for geodynamics, seismic hazard and civil protection goals. The network considered in this work is constituted by 6 stations (fig. 1b). The number of vertices is rapidly increasing over the Italian region, either in correspondence of the new and old INGV seismic stations or independently from them. The GPS monuments are realized by means of reinforced concrete pillars, linked to the coherent rock outcrops or deeply anchored in non consolidated deposits. The GPS antenna is connected to the pillar by means of two different devices: the INGV-3D antenna mount (http://www.ingv.it/labtel2/ufpage.htm) and the SCIGN antenna mount (http://jacinto.ucsd.edu/gpsmon/adaptor_design/intro.html). For some of the stations the raw data are daily transferred on a server, for other, where telemetric connection is still not available, the raw data are downloaded locally and later archived.

FREDNET – The Friuli Regional Deformation Network (FREDNET; http://www.crs.inogs.it/

frednet/) is operated and maintained by the Centro Ricerche Sismologiche (CRS) of the Istituto Nazionale di Oceanografia e di Geofisica Sperimentale, in Udine. The network has been installed to monitor crustal deformation along the northeastern boundary of the Adriatic microplate. The goal is to estimate interseismic strain accumulation on active faults for a better assessment of the regional seismic hazards, but also to provide infrastructure for geodetic data management and processing. The network is presently constituted by 8 stations, characterized by high and uniform construction standards. Most of the stations are built on stable rock outcrops (with the exception of UDIN and TRIE, which are located on buildings) and all are equipped with the same GPS equipment. The choke-ring antennas, covered with a SCIGN dome, are mounted on a 1-m reinforced concrete pillar founded in the surface bedrock by means of epoxied metal rods. Since most of the stations are located in remote areas, cellular modems are used to send the data to the local archive. All the data of this network are routinely analyzed.

REGAL – The Réseau GPS permanent dans les Alpes network (REGAL; http://kreiz.unice.fr/regal/) is a permanent GPS array located in the Western Alps and their surroundings. The network, which is dedicated to crustal deformation monitoring (Calais *et al*., 2000), started operating in 1997 and currently consists of 22 stations, some of which contributes to the France RGP (Reseau GPS Permanent) and EUREF networks. The REGAL station monuments are mainly concrete pillars founded on stable bedrock, equipped with choke-ring antennas. We analyze data from 7 stations, selected considering their data availability trough time and their monumentation quality.

AUSTRIA – The Austrian Continuous GPS Network is constituted by more than 35 stations, some of them contributing to the EUREF network, and is operated by the Department of Satellite Geodesy of the Austrian Accademy of Science (http://www.iwf.oeaw.ac.at/english/research/earth/geodynamics/gps_e.html). This network has been established to investigate geodynamic processes in the Eastern Alpine region, but also for commercial applications, such as mapping and cadastral purposes. We do not process observations from the whole network, but we analyze data from 5 sites selected using as criteria the data availability trough time and the monument quality (when available as information on the web site).

OTHER – Other CGPS stations are currently operating in the Italian region. Some of them have been installed in the frame of national projects (*i.e.*, CADM), some other are maintained by University departments (ASIA, BASO, BRAS and ROVI), or by Administrative agencies (MERA and TREN).

3. RINEX data archiving

In order to manage the large amount of data coming from the CGPS networks considered, we developed several procedures, under Linux operating system, to set up an archive for RINEX data and meta-data (*i.e.*, orbits) files. We used the File Transfer Protocol (FTP), automated by means of Bourne Shell (BASH) and Enhanced Courne Shell (CSH, TCSH) scripts and FORTAN77 programs, to download and archive RINEX files from remote ftp archives and to check antenna/receiver inconsistencies. This is crucial to maintain a database of observations that follows the IGS standards, and to build a historical record of stations equipment changes.

Figure 2 displays a flow-chart of the data archiving steps. On a weekly basis, we download RINEX data from several remote FTP archives (listed in table I), and archive them, together with orbits (precise and broadcast) and station information (*i.e.*, station log-files). Considering that some of the sites collected display inconsistencies and errors in their RINEX file headers (*e.g.*, wrong antenna/receiver codes and/or wrong antenna heights), which can significantly affect the data processing or further interpretations, an important module of the archiving procedures is devoted to the detection and correction of such errors to IGS standards (ftp://igscb.jpl.nasa.gov/igscb/data/format/rinex210.txt). To perform this task we developed several automated programs, both using FORTAN77 and BASH, which make use of the Unavco-TEQC software for GPS data and meta-data handling (http://www.unavco.org/facility/software/teqc/teqc.html).
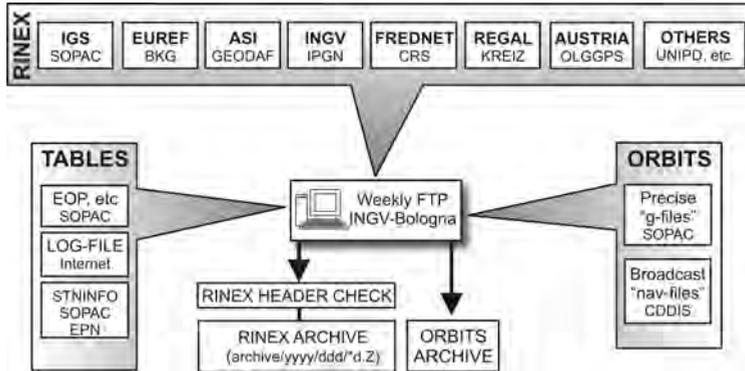
Fig. 2. Flow chart of the CGPS data archiving procedures.

Station information required to process and interpret GPS observations are obtained for most of the stations from the *station.info* table (ftp://lox.ucsd.edu/gamit/table), a machine readable file that lists the equipment history (*i.e.*, receiver, antenna, offsets, agencies, domes, firmware, and the epochs of any change in the station configuration) of all the CGPS stations archived and processed by the Scripps Orbit and Permanent Array Center (SOPAC; http://sopac.ucsd.edu) of the University of California in San Diego. This file is derived by a daily analysis, through the SOPAC's Oracle Relation Database Management System (RDBMS), of all the standard log-files archived at SOPAC. For other sites not included into the SOPAC data base, these information are retrieved from EUREF-EPN historical station equipment configuration summary file (available at http://www.epncb.oma.be/tp/station/general/extlog.hst) or directly from the station-log-files.

It is worth noting that some of the CGPS stations considered in this work (labeled as LOCAL in table I) are currently collecting data locally, and do not transmit data to remote archives. For this reason their RINEX files are checked and archived only when available. For some other stations the RINEX data are not freely available on the Internet, and we process these data in agreement with the local operating institutions (labeled as CONV in table I).

At the end of the archiving procedure, the standard RINEX files are compressed, using the Hatanaka format (http://igscb.jpl.nasa.gov/mail/igsmail/1998/msg00012.html), and stored in the archive, which is maintained on a weekly basis. Ancillary data required to analyze the GPS phase observations, including broadcast ephemeredes and apriori orbits, stations coordinates and velocities, Earth orientation parameters, UT1 and Leap Second tables, are retrieved weekly from CDDIS (ftp://cddisa.gsfc.nasa.gov/) and SOPAC archives. All files are collected weekly, just prior to subsequent processing, and stored in the orbits and tables archives (see fig. 2). We use the final SOPAC orbits (in *g*-file format, the internal GAMIT format), instead of the final IGS orbits, in order to maintain the highest homogeneity and uniformity in combining our solutions with the SOPAC regional and global ones.

4. CGPS data processing

Determining a self consistent set of station velocities from a vast amount of space geodetic data requires methods for reducing the large number of raw GPS observations to geodetic parameter estimates, such as site positions and velocities, Earth orientation parameters, satellite orbital parameters, and methods for combining the results to form a set of velocities in a uniform reference frame. The technique of CGPS is severely affected by problems of data volume and data consistency and, computationally, it is not

feasible to treat all of the data available from the hundreds of stations operating in the Mediterranean and European region on any given day simultaneously. Over the last few years, however, some techniques have been developed to make efficient use of the ever growing GPS data set using the computational resources available (Blewitt *et al*., 1993). These techniques, which are defined as «distributed processing» approach, also provide a convenient means of combining results from different space geodetic techniques (*i.e.*, Dong *et al*., 1998), such as VLBI, SLR, and campaign GPS measurements, while preserving uniformity in the reference frame definition. The basic approach is to analyze the data in subnetworks (clusters of stations), and then combine the subnetwork solutions using procedures analogous to sequential least squares (*i.e.*, Kalman filter). Because subnetworks are processed separately, this strategy also allows to combine the reduced data products derived from different techniques and by different analysts at different institutions, saving a very large amount of time and effort. The SOPAC facility routinely analyzes, starting from 1991, RINEX data coming from several CGPS networks all over the world, including the entire IGS network, and a sub-set of EUREF-EPN stations. The SOPAC facility provides the scientific community with daily loosely constrained solutions for all the networks they archive, and we took advantage of the distributed processing mode by not processing stations already analyzed by SOPAC, but choosing a set of IGS and EUREF stations that are shared by our three regional subnetworks and SOPAC global/regional ones (stations reported in fig. 1a,b with black squares, plus NYA1 that is outside the map).

Another important feature of the distributed processing approach is that the reference frame is not defined until the last step of the analysis. This is achieved by applying loose constraints to all parameters (site positions, satellite orbital parameters, Earth orientation parameters) when reducing the raw data such that reference frame indeterminacy is regularized, but without affecting the invariant properties of the parameters estimates (*i.e.*, Herring *et al*., 1991; Heflin *et al*., 1992). Moreover, this approach, based on the «*quasi*-observation» theory (Dong *et al*., 1998),

allows for a rigorous combination of CGPS and non-permanent networks. Hence, different analysts can share data products without having to worry about the particular values the other analysts adopted to define their reference frames. Although we do not «fix» orbital and Earth orientation parameter estimates to precise values, we do use precise values for these parameters provided by the SOPAC facility as it benefits data editing and analyses.

The RINEX data coming from more than 80 stations (table I) are routinely processed using the GAMIT/GLOBK software (King and Bock, 2000), installed on two Linux machines, equipped with Intel-Pentium 4 processors and 1 GB of RAM memory, and a SUN-Ultrasparc station. Considering that the stations analyzed are equipped with largely different GPS instruments (*i.e.*, different receivers and antennas), building clusters using the GPS equipment as criteria, which would be the best solution in order to avoid antenna mixing, is not feasible with the computational facilities available. For this reason we first used a geographical criteria, dividing the network into two main subnetworks, a northern and a southern one. We then set-up a third cluster for all the stations that display lower regularity in the data availability, or that, in previous analysis, displayed lower data quality. Table I shows the clusters to which each station belongs.

Our raw data analysis procedure is divided into three main steps that include the phase data analysis, the combination of solutions and the position time-series analysis (fig. 3). Each step is performed by means of three different software packages. The same processing scheme is applied uniformly to each day of the 5 years analysis considered in this work, but considering that changes in weighting schemes and software versions are thought to have minimal effects on the coordinate time-series. At the end of the three steps we obtain three dimensional displacement rates in the most recent release of the ITRF frame.

4.1. *Raw data reduction*

The first step is performed through the GAMIT module, which uses double-differ-
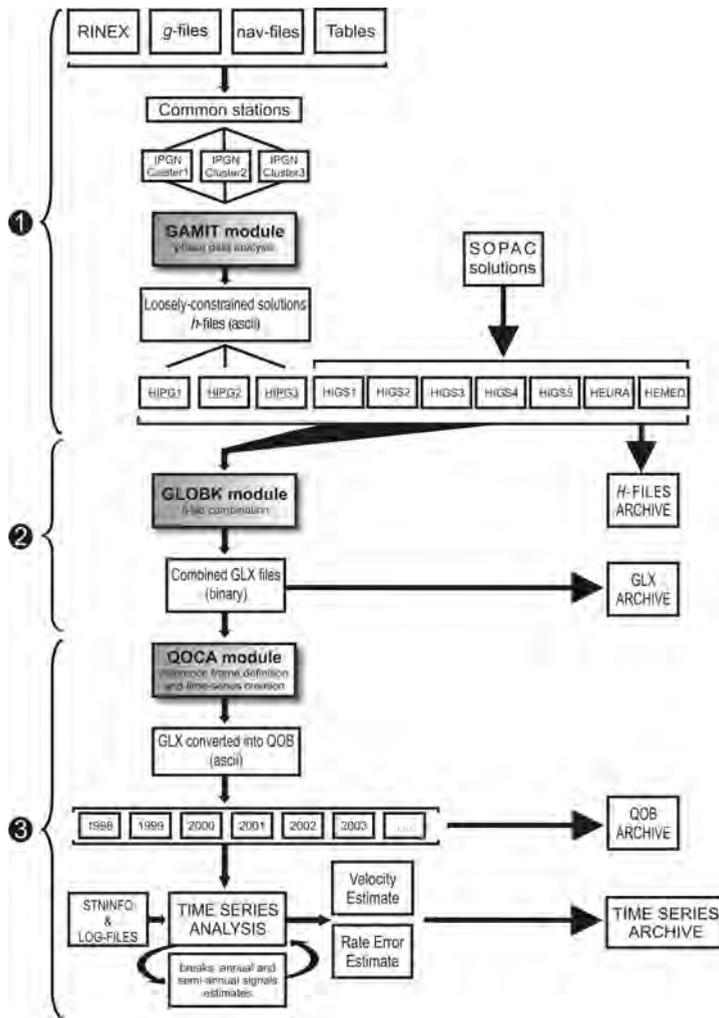
Fig. 3. Flow chart of the CGPS data processing steps.

enced, ionosphere-free linear combinations of the $L1$ and $L2$ phase observations to generate weighted least square solutions for each daily session (King *et al.*, 1985; Bock *et al.*, 1986; Schaffrin and Bock, 1988; Dong and Bock, 1989). An automatic cleaning algorithm (AU-TOCLN; for more details see Herring, 2000; King and Bock, 2000) is applied to postfit residuals, in order to repair cycle slips and to remove outliers; no attempt is usually made to recover

edited data using manual techniques. The observation weights vary with elevation angle and are successively derived individually for each site from the scatter of postfit residuals obtained in a preliminary solution. Estimated parameters for each daily solution include the 3D Cartesian coordinates for each site, 6 orbital elements for each satellite (semi-major axis, eccentricity, inclination, longitude of ascending node, argument of perigee, and mean anomaly), Earth ori-

entation parameters (pole position and rate and UT1 rate), and integer phase ambiguities (more details about bias-fixing procedures can be found in Serpelloni *et al.*, 2002). We also estimate hourly piecewise-linear atmospheric zenith delays at each station to correct the poorly modeled troposphere, and 3 east-west and north-south atmospheric gradients per day, to account for azimuthal asymmetry; the associated error covariance matrix is also computed and saved. The elevation cutoff is set to 10° and we use the IGS elevation dependent models for modeling the effective phase center of the receiver antennas. The effect of solid-earth tides, polar motion and oceanic loading are taken into account. Diurnal, semidiurnal and long period tide components are modeled according to the IERS/IGS standard 1996 (IERS Tech. Notes, 21, 1996). The correction for the polar motion are computed following the IERS convention (McCarthy, 1996); the largest period modeled is the Chandler Wobble (about 460 days). The oceanic loading correction is based on the Scherneck model (Scherneck, 1991), where amplitudes and phase of 11 components are determined.

The three subnetworks (see table I) are processed in parallel, with 11 overlapping «tie» sites included in each cluster, to provide a means of combining the individual solutions later in GLOBK, and also with the solutions given by SOPAC.

The basic products of this step are loosely-constrained solutions for each subnetwork, containing set of one-day site position estimates, Earth orientation parameters, and associated error covariance matrices. For the second step of the analysis it is also convenient to save in addition the satellite orbital parameter estimates. These data products, together with the loosely-constrained «*h*-file» solutions provided by SOPAC for the IGS1, IGS2, IGS3, IGS4, IGS5, EURA and EMED subnetworks (more information can be found at the SOPAC web page: http://sopac.ucsd.edu/processing/gamit/), are stored in the ASCII «*h*-file» format to form the *h*-file archive (see fig. 3). In the following discussion we refer to the vector of parameter estimates derived from the raw data from the *k*th subnetwork as h_k, with H_k denoting the associated variance-covariance matrices.

4.2. *Combination of loosely constrained solutions*

Once the loosely-constrained GPS parameter estimates from the individual GAMIT solutions (h_k, H_k) are obtained from the analysis of each subnetwork, these are combined using the GLOBK software (Herring, 2000) to form a daily unconstrained combined network solution (h_T, H_T). As in all intermediate steps, in our procedures the reference frame is only loosely defined in forming these combined network solutions. We effectively achieve this by solving the system of equations

$$h_1 = A_1 h_T + e_1$$
$$h_2 = A_2 h_T + e_2$$
$$\vdots$$
$$h_k = A_k h_T + e_k$$

where k is the total number of subnetworks being combined (in this case 10), A_k are design matrices which related the total parameter set h_T to the *k*th subset h_k, and e_k represent the errors in the estimates h_k such that $\mathrm{E}e_k e_k^T = H_k$, where E is the mathematical expectation operator. The h_T vector contains estimates for the site positions and Earth orientation parameters at the epoch *T*. We compute one total network solution for each day, which is stored in the binary GLX format (binary GLOBK format for the loosely-constrained bias-fixed solutions) and archived (see fig. 3). These files are thus converted into ASCII QOB (*Quasi*-OBservation) file format, and stored in the QOB archive (see fig. 3). It is worth noting that after combination into total network solution, we no longer need and retain the satellite orbital parameter estimates. A more detailed description of the mathematics involved in data combination and specific implementation in the GLOBK software can be found in Herring *et al.* (1990), Dong *et al.* (1998), and Herring (2000).

One of the main advantages of the adopted processing scheme is that the obtained QOB files carry the position time-series of all the CGPS stations included into the subnetworks we combined, that is more than 320 sites, distributed all over the Earth's surface. This allows
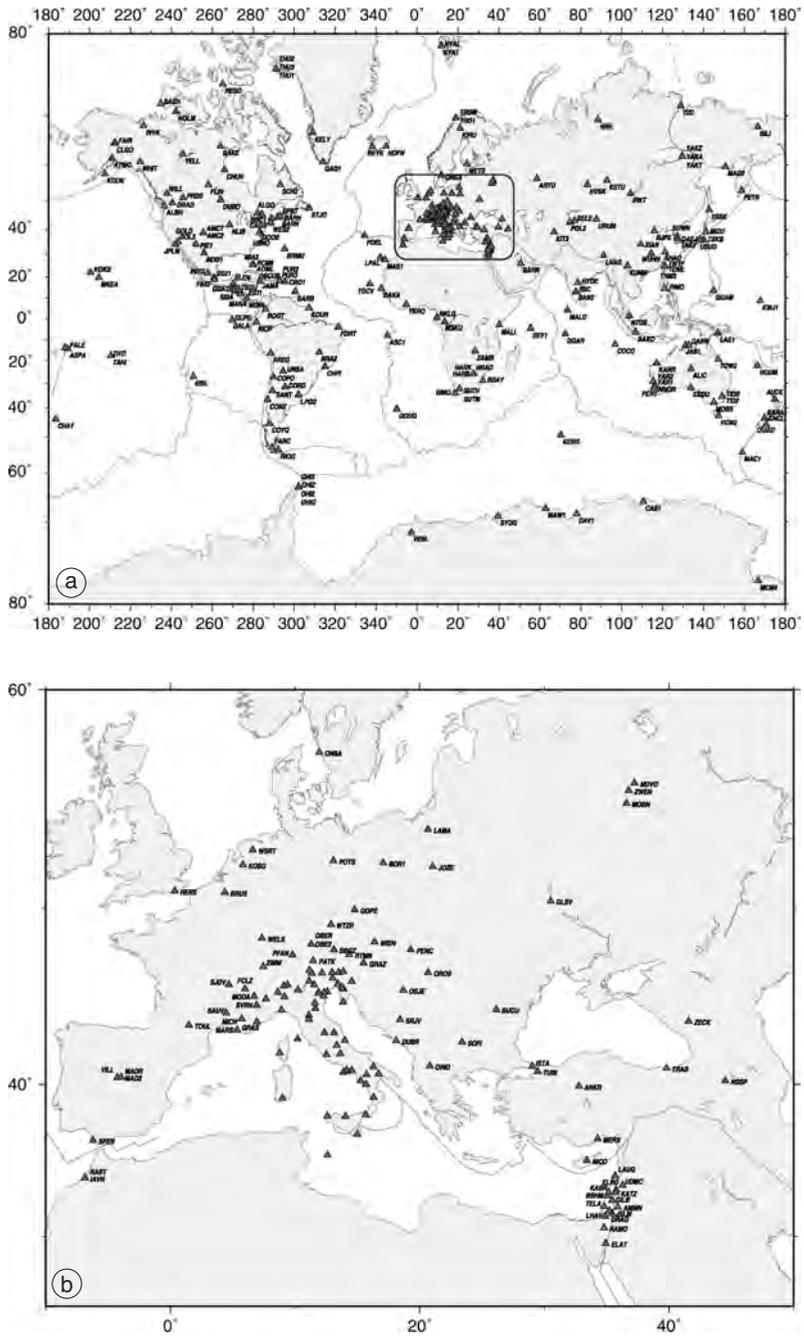
Fig. 4a,b. Maps of the full CGPS network that is obtained from the combination of our three regional solutions with the SOPAC loosely constrained solutions. Position time-series, and three dimensional velocities, are available for all the stations displayed.

for further tectonic studies at different scales, from the local fault segment scale to the global plate motion scale, using a uniform and self-consistent set of three dimensional station velocities. Figure 4a,b displays the sites for which we have position time-series available.

4.3. *Position time series analysis and velocity estimate*

The loosely constrained daily combined solutions (in ASCII QOB format) are input as *quasi-observations* to the *Quasi*-Observation Combination Analysis (QOCA) software (available at http://gipsy.jpl.nasa.gov/qoca), which is used to define a common reference frame, deriving the position time-series for all the stations. For each daily QOB file the network constraint solution (see Dong *et al.*, 1998, Appendix C) is constructed using the 50 globally distributed core sites listed in table II. A seven-parameter transformation (three network rotations, three network translations, and one scaling parameter) is performed, aligning each solution to the 2000 realization of the International Terrestrial Reference Frame (Altamimi, 2002).

The set of stations used to define the global reference frame is chosen to provide optimal global stability over time, but not only over the time interval considered in this work. In fact,

since the current network of IGS core sites was not complete until 1997 and one of our goals is also to combine continuous and non permanent GPS observations from the early nineties (Serpelloni *et al.*, 2002) as uniformly as possible, the IGS core sites are supplemented with other stations (table II) characterized by a very long history and good quality data, and with positions and velocities well-determined in the ITRF2000, or at least in the ITRF97. For the selected core stations we assume rates equal to the current site rates estimated in the ITRF2000 solution (Altamimi *et al.*, 2002). Since the vertical coordinates usually have poorer accuracy than the horizontal ones, we reduced the weight of vertical positions at core sites by a factor 100, in determining the 7 network parameters.

The observed motion $f(t)$ of each site in each direction (north, east, up) can be written as (*e.g.*, Ding *et al.*, 2005)

$$f(t_i) = a + bt_i + c\sin(2\pi t_i) + d\cos(2\pi t_i) +$$
$$+ e\sin(4\pi t_i) + f\cos(4\pi t_i) + \sum_{j=1}^{n_g} g_j H(t_i - T_g) + \varepsilon_i$$

where t_i for $i=1, \ldots, N$ are the daily solutions epochs in units of years, and H is the Heaviside step function (Abramowitz and Stegun, 1972). The first two terms are the constant bias with

Table II. List and coordinates of the 50 global and regional tracking stations used to apply the internal constraints in the reference frame definition.

Station	Long	Lat	Station	Long	Lat	Station	Long	Lat	Station	Long	Lat	Station	Long	Lat
ALBH	−123.49	48.39	GRAS	6.92	43.76	MAC1	158.94	−54.50	PERT	115.89	−31.80	TRO1	18.9	69.7
ALGO	−78.07	45.96	GRAZ	15.49	47.07	MALI	40.19	−3.00	PIE1	−108.12	34.30	TSKB	140.1	36.1
BOR1	17.07	52.28	GUAM	144.87	13.59	MAS1	−15.63	27.76	POTS	13.07	52.38	USUD	138.4	36.1
BRMU	−64.70	32.37	HARK	27.71	−25.89	MATE	16.70	40.65	REYK	−21.96	64.14	VILL	−4.0	40.4
BRUS	4.36	50.80	HERS	0.34	50.87	MDO1	−104.02	30.68	SHAO	121.20	31.10	WES2	−71.5	42.6
CAGL	8.97	39.14	IRKT	104.32	52.22	METS	24.40	60.22	STJO	−52.68	47.60	WETT	12.9	49.1
DAV1	77.97	−68.58	JOZE	21.03	52.10	NLIB	−91.58	41.77	TELA	34.78	32.07	WTZR	12.9	49.1
DRAO	−119.63	49.32	KERG	70.26	−49.35	NYAL	11.87	78.93	TIDB	148.98	−35.40	YAR1	115.3	−29.0
FORT	−38.43	−3.88	KOKB	−159.67	22.13	NYA1	11.87	78.93	TOUL	1.48	43.56	YELL	−114.5	62.5
GOLD	−116.89	35.43	KWJ1	167.73	8.72	ONSA	11.93	57.40	TROM	18.94	69.66	ZIMM	7.5	46.9

Table III. Amplitudes of the annual, semi-annual signals and offsets detected from the analysis of position time-series of stations that observed more than 3 years. For each station (ID code), the observation interval (ΔT), the annual and semiannual cosine and sine amplitudes (in mm), the weighted RMS, the epochs of breaks in the time-series and the related offsets are listed for the north, east and vertical components. One standard deviation errors are also given.

Station name	Component	Annual Cos (mm)	Annual Sin (mm)	Semiannual Cos (mm)	Semiannual Sin (mm)	WRMS mm	Offsets d/m/yr	mm	d/m/yr	mm	d/m/yr	mm
AJAC	North	0.40±0.06	0.77±0.06	-0.07±0.06	-0.63±0.06	1.43						
ΔT (yr)	East	-0.34±0.08	-0.07±0.08	0.33±0.08	-0.10±0.08	1.86						
3.3648	Up	-2.08±0.18	1.63±0.17	0.21±0.17	-0.33±0.17	4.09						
AQUI	North	0.19±0.06	0.79±0.07	-0.02±0.07	-0.25±0.06	1.77	27/08/2001	0.76±0.17				
ΔT (yr)	East	-0.56±0.08	0.67±0.08	0.40±0.08	-0.21±0.07	2.02	27/08/2001	3.75±0.21				
4.547	Up	-3.00±0.21	-1.12±0.21	0.41±0.21	1.03±0.20	5.6	27/08/2001	-7.40±0.54				
BRAS	North	-0.18±0.07	-0.32±0.07	-0.04±0.07	-0.39±0.07	1.77						
ΔT (yr)	East	-0.49±0.06	-0.29±0.06	0.19±0.06	-0.09±0.06	1.65						
3.5948	Up	-4.06±0.19	-1.43±0.19	0.29±0.19	-0.01±0.19	4.71						
BZRG	North	1.44±0.05	0.36±0.06	0.00±0.05	-0.13±0.05	1.58	29/11/2000	3.81±0.16				
ΔT (yr)	East	-0.06±0.07	-0.37±0.07	0.01±0.06	-0.32±0.06	1.85	29/11/2000	-2.06±0.21				
5.9959	Up	-2.99±0.18	-1.78±0.18	-0.03±0.18	-0.04±0.18	5.17	29/11/2000	-20.12±0.52				
CADM	North	0.26±0.08	0.34±0.08	0.56±0.08	0.05±0.07	1.29						
ΔT (yr)	East	-1.75±0.11	-1.00±0.12	0.65±0.11	0.33±0.10	1.77						
3.1786	Up	-3.18±0.29	0.73±0.30	1.61±0.28	1.22±0.26	4.56						
CAGL	North	-0.56±0.05	-0.15±0.05	0.06±0.05	-0.02±0.05	1.54	11/07/2001	-1.36±0.13				
ΔT (yr)	East	-1.89±0.07	-0.64±0.07	0.13±0.07	-0.04±0.07	2.14	11/07/2001	4.22±0.20				
5.8617	Up	-2.72±0.17	2.04±0.17	0.40±0.17	-0.48±0.17	5.28	11/07/2001	0.35±0.46				
CAME	North	-0.35±0.09	0.16±0.09	-0.09±0.08	-0.15±0.08	1.57	15/12/2003	1.27±0.35				
ΔT (yr)	East	-0.81±0.11	-0.61±0.11	0.23±0.10	-0.07±0.10	2.08	15/12/2003	3.11±0.41				
3.6769	Up	-0.71±0.32	-0.32±0.30	0.99±0.28	-0.54±0.28	6.06	15/12/2003	11.29±1.27				
COSE	North	0.12±0.09	0.22±0.10	0.50±0.09	-0.02±0.10	1.44						
ΔT (yr)	East	-0.90±0.14	0.18±0.15	0.33±0.14	0.20±0.16	2.22						
3.3484	Up	-1.98±0.37	2.93±0.38	-0.86±0.37	0.33±0.40	5.65						
DUBR	North	-1.05±0.07	-0.77±0.07	-0.48±0.07	0.00±0.07	1.61						
ΔT (yr)	East	-0.36±0.08	0.88±0.08	0.30±0.08	-0.35±0.08	1.74						
3.2745	Up	-3.97±0.19	-0.55±0.19	0.28±0.18	0.90±0.18	4.1						
ELBA	North	0.21±0.07	0.28±0.07	-0.15±0.07	-0.48±0.07	1.62						
ΔT (yr)	East	-0.28±0.09	-0.24±0.09	0.02±0.09	-0.27±0.09	2.05						
3.1431	Up	-3.23±0.23	-0.85±0.24	0.88±0.23	-0.84±0.23	5.33	30/03/2003	5.39±0.58				
GENO	North	0.57±0.05	0.54±0.05	0.08±0.05	-0.22±0.05	1.61						

Table III (*continued*).

Station name ΔT (yr)	Component	Annual Cos (mm)	Annual Sin (mm)	Semiannual Cos (mm)	Semiannual Sin (mm)	WRMS (mm)	Offsets d/m/yr	mm	d/m/yr	mm	d/m/yr	mm
ΔT (yr) 5.4428	East	−0.10±9.06	0.17±0.06	0.14±0.06	−0.41±0.06	1.8						
	Up	−2.35±0.17	−0.21±0.17	−1.19±0.17	−0.03±0.17	5.23						
GRAS ΔT (yr) 5.8261	North	0.01±0.04	0.61±0.04	0.25±0.04	−0.33±0.04	1.15						
	East	−0.33±0.06	0.17±0.05	0.15±0.05	−0.33±0.05	1.59						
	Up	−1.42±0.13	0.61±0.13	−0.43±0.12	−0.93±0.13	3.6						
GRAZ ΔT (yr) 5.9959	North	0.15±0.03	−0.10±0.03	0.17±0.03	0.17±0.03	0.97	23/04/2003	−0.83±0.12	07/05/2001	−1.46±0.10	−1.46±0.10	−1.46±0.10
	East	0.08±0.04	0.00±0.04	0.08±0.04	−0.25±0.04	1.31	23/04/2003	2.61±0.14	07/05/2001	−2.30±0.14		
	Up	−3.48±0.13	−0.68±0.12	0.06±0.12	0.10±0.12	3.71	23/04/2003	3.74±0.37	07/05/2001	−0.68±0.38		
INGR ΔT (yr) 3.5975	North	0.42±0.07	0.78±0.07	−0.23±0.06	−0.16±0.07	1.5						
	East	2.58±0.08	1.20±0.08	0.27±0.08	−0.23±0.08	1.88						
	Up	−2.91±0.20	−1.02±0.21	0.72±0.19	0.08±0.19	4.48	01/07/2000	4.20±0.37				
LAMP ΔT (yr) 4.7666	North	−0.70±0.06	0.030±0.06	−0.12±0.06	−0.22±0.06	1.61						
	East	−1.06±0.07	−0.03±0.07	0.37±0.07	−0.35±0.07	2.07						
	Up	−2.87±0.18	2.57±0.18	1.13±0.18	0.49±0.18	5.1	25/01/2002	−9.66±0.60	28/05/2002	9.29±0.62		
MATE ΔT (yr) 5.9959	North	−0.04±0.04	−0.05±0.04	0.07±0.04	−0.11±0.04	1.26	18/06/1999	−3.10±0.12				
	East	0.44±0.05	−0.13±0.05	0.04±0.05	0.08±0.05	1.6	18/06/1999	3.75±0.16				
	Up	−3.18±0.12	0.10±0.13	0.11±0.12	0.59±0.12	3.98	18/06/1999	3.27±0.39	22/08/2002	−5.59±0.36		
MEDI ΔT (yr) 5.9959	North	−0.22±0.05	−0.91±0.05	0.29±0.05	0.17±0.05	1.51	03/04/2001	−3.78±0.14				
	East	−0.01±0.07	1.18±0.06	0.13±0.06	−0.49±0.07	1.96	03/04/2001	0.10±0.20				
	Up	−3.94±0.15	0.01±0.14	−0.35±0.14	0.36±0.14	4.27	03/04/2001	−7.40±0.40				
NOT1 ΔT (yr) 3.3128	North	0.62±0.07	0.96±0.07	−0.24±0.07	−0.31±0.07	1.62						
	East	−1.44±0.10	−0.22±0.10	−0.17±0.10	−0.09±0.10	2.4						
	Up	−2.08±0.23	1.16±0.23	0.34±0.23	0.40±0.23	5.38						
NOVA ΔT (yr) 3.5318	North	1.65±0.07	0.42±0.08	−0.15±0.07	−0.00±0.07	1.44						
	East	−0.45±0.07	−0.12±0.09	0.19±0.08	−0.05±0.07	1.5						
	Up	−2.60±0.20	1.12±0.22	−1.26±0.21	−0.20±0.21	4.23						
OBER ΔT (yr) 3.4634	North	−0.07±0.04	0.06±0.04	0.49±0.04	0.16±0.04	0.99						
	East	−0.29±0.06	0.07±0.06	0.11±0.06	−0.07±0.06	1.33						
	Up	−1.97±0.17	−0.09±0.16	−0.39±0.16	0.33±0.16	3.76						
ORID ΔT (yr) 3.4661	North	−0.10±0.06	0.08±0.07	−0.14±0.06	−0.10±0.06	1.24						
	East	0.07±0.09	−0.36±0.10	0.30±0.09	−0.17±0.09	1.8						
	Up	−1.99±0.25	−2.05±0.28	−0.36±0.24	0.86±0.25	4.65						
OSJE	North	−0.75±0.05	0.46±0.05	0.11±0.05	−0.09±0.05	1.17						

Table III (*continued*).

Station name / ΔT (yr)	Component	Annual Cos (mm)	Annual Sin (mm)	Semiannual Cos (mm)	Semiannual Sin (mm)	WRMS (mm)	d/m/yr	mm	d/m/yr	mm	d/m/yr	mm	d/m/yr	mm
ΔT (yr) 3.2827	East	−0.56±0.07	−0.28±0.07	0.11±0.07	−0.10±0.07	1.59								
	Up	−1.74±0.13	−3.41±0.19	−0.04±0.18	0.38±0.18	4.2								
PRAT ΔT (yr) 5.6509	North	−0.19±0.07	−0.15±0.07	0.23±0.07	0.20±0.07	1.97								
	East	−0.27±0.06	0.47±0.06	0.20±0.06	−0.14±0.06	1.68								
	Up	−2.28±0.17	0.10±0.17	−0.59±0.17	0.09±0.17	4.97								
SRJV ΔT (yr) 4.46	North	0.55±0.09	1.04±0.09	0.06±0.08	−0.17±0.08	1.68								
	East	0.06±0.09	0.17±0.11	−0.31±0.09	−0.39±0.09	1.75								
	Up	−2.48±0.25	1.38±0.27	0.24±0.24	0.20±0.24	4.82	14/06/2003	9.95±0.62						
TGRC ΔT (yr) 3.4497	North	−0.52±0.09	−0.02±0.09	−0.10±0.09	−0.04±0.09	2.08								
	East	−0.52±0.14	0.30±0.14	0.92±0.14	0.40±0.14	3.28								
	Up	−2.52±0.31	1.18±0.32	0.83±0.32	2.40±0.31	7.24								
TORI ΔT (yr) 5.7851	North	−1.10±0.05	0.17±0.05	−0.02±0.05	0.06±0.05	1.42								
	East	1.01±0.06	0.05±0.06	0.01±0.06	−0.20±0.06	1.74								
	Up	−3.79±0.18	−1.01±0.18	0.25±0.18	0.25±0.18	5.35								
UNPG ΔT (yr) 5.7851	North	−0.44±0.05	−0.19±0.05	0.31±0.05	0.01±0.05	1.36								
	East	0.38±0.06	0.05±0.06	0.27±0.06	−0.33±0.06	1.74								
	Up	−2.95±0.17	0.91±0.16	−0.20±0.16	−0.01±0.16	4.63	19/05/2002	−7.33±0.16	23/11/1998	−18.48±0.48	10/02/2000	10.33±0.50	25/11/2000	5.15±0.51
UPAD ΔT (yr) 3.8741	North	0.99±0.06	−0.02±0.05	0.14±0.06	0.17±0.05	1.32								
	East	−1.32±0.07	−0.77±0.06	0.30±0.07	0.19±0.06	1.54								
	Up	−3.49±0.19	1.35±0.18	−0.72±0.18	0.14±0.18	4.31								
VENE ΔT (yr) 5.9959	North	2.40±0.06	0.84±0.07	0.59±0.06	−0.96±0.06	1.83								
	East	−1.78±0.06	−1.38±0.06	0.13±0.06	0.56±0.06	1.68	01/02/2001	3.20±0.17						
	Up	−4.00±0.20	0.22±0.23	−0.08±0.20	0.29±0.20	5.84	01/02/2001	1.13±0.17	22/08/1999	−52.99±0.68	01/02/2001	94.53±0.64	15/12/2001	10.34±0.54
VLUC ΔT (yr) 5.4073	North	−0.66±0.08	0.28±0.08	0.15±0.08	−0.03±0.08	1.71								
	East	−0.24±0.10	−0.47±0.10	0.35±0.10	−0.00±0.10	2.16								
	Up	−4.83±0.24	−0.79±0.24	0.91±0.24	1.22±0.23	5.14								
VVLO ΔT (yr) 3.5838	North	−0.65±0.08	0.49±0.09	−0.00±0.09	0.06±0.09	1.92	31/08/2001	−2.36±0.27	11/01/2003	1.09±0.26				
	East	0.28±0.09	0.03±0.10	−0.29±0.10	−0.09±0.09	2.11								
	Up	−2.76±0.26	−0.14±0.27	1.38±0.27	1.64±0.26	5.9	31/08/2001	−2.00±0.82	11/01/2003	5.70±0.79				
ZIMM ΔT (yr) 5.9959	North	−0.10±0.03	−0.15±0.03	0.09±0.03	0.02±0.03	1.06	06/11/1998	0.98±0.10						
	East	−0.31±0.04	−0.03±0.05	−0.02±0.04	−0.31±0.04	1.41	06/11/1998	3.01±0.13						
	Up	−1.62±0.12	−0.58±0.12	−0.58±0.12	−0.39±0.12	3.78	06/11/1998	−11.63±0.3						

914

respect to 1998.00, *a*, and the linear rate, *b*, respectively. Coefficients *c* and *d* describe the annual periodic motion, while *e* and *f* describe the semi-annual motion. The next term corrects for any number (n_g) of offsets, with magnitudes *g*

and epochs T_g. In some time-series there are offsets due mainly to antenna or receiver changes, which we model as step functions. Assuming that the offset epochs are known, the model is linear with respect to the coefficients.

Table IV. Velocity values and 1σ uncertainties for the CGPS stations that observed for more than three years. Residual horizontal velocities are given with respect to the Eurasian frame of Serpelloni *et al.* (2005), and residual vertical velocities are given with respect to the Corsica-Sardinia block.

Site	Velocity (mm/yr)		Uncertainty (mm/yr)		Residual velocity (mm/yr)		Velocity (mm/yr)	Uncertainty (mm/yr)	Residual velocity (mm/yr)
ID	East	North	East	North	East	North	Vertical	Vertical	Vertical
AJAC	21.11	14.69	0.55	0.58	−0.12	−0.40	−0.60	1.32	0.60
AQUI	20.72	15.69	0.48	0.49	−1.23	1.18	0.56	1.01	1.76
BRAS	21.81	16.08	0.54	0.57	0.56	1.28	1.08	1.26	2.28
BZRG	19.67	14.61	0.41	0.42	−1.18	−0.16	0.82	0.79	2.02
CADM	23.66	18.17	0.57	0.59	1.03	4.08	0.75	1.45	1.95
CAGL	21.85	15.28	0.42	0.44	0.12	0.21	−1.80	0.82	−0.60
CAME	22.42	17.19	0.59	0.61	0.63	2.65	−2.91	1.49	−1.71
COSE	23.66	16.65	0.55	0.57	0.76	2.57	−3.20	1.40	−2.00
DUBR	22.40	16.84	0.56	0.58	−0.30	3.04	−1.16	1.35	0.04
ELBA	20.76	15.10	0.57	0.60	−0.58	0.19	−0.60	1.40	0.60
GENO	21.11	14.87	0.43	0.44	0.31	−0.20	−1.09	0.85	0.11
GRAS	20.86	15.38	0.42	0.43	0.30	0.09	−2.02	0.82	−0.82
GRAZ	22.29	14.64	0.41	0.42	0.79	0.44	−1.52	0.80	−0.32
INGR	22.02	16.21	0.53	0.55	0.13	1.59	−0.79	1.24	0.41
LAMP	20.33	17.74	0.46	0.48	−2.47	3.13	−0.15	0.96	1.05
MATE	23.85	18.46	0.41	0.43	1.09	4.44	1.08	0.80	2.28
MEDI	22.81	17.50	0.41	0.42	1.53	2.77	−2.69	0.79	−1.49
NOT1	21.69	18.75	0.56	0.59	−1.30	4.47	−0.95	1.35	0.25
NOVA	20.14	14.89	0.53	0.55	−0.41	−0.21	−0.09	1.28	1.11
ORID	24.46	9.72	0.58	0.60	1.13	−3.65	−1.94	1.46	−0.74
OSJE	22.01	14.05	0.56	0.58	−0.32	0.34	−2.34	1.36	−1.14
PRAT	22.16	17.12	0.42	0.44	0.87	2.32	−2.09	0.83	−0.89
SRJV	22.95	15.16	0.56	0.58	0.39	1.41	0.75	1.38	1.95
TGRC	24.12	16.27	0.55	0.57	1.18	2.09	−0.23	1.31	0.97
TORI	20.87	15.01	0.42	0.43	0.43	−0.20	−0.72	0.82	0.48
UNPG	21.93	15.94	0.42	0.43	0.28	1.30	0.40	0.82	1.60
UPAD	21.61	16.87	0.51	0.53	0.46	2.17	−3.61	1.17	−2.41
VENE	22.22	15.47	0.41	0.42	0.99	0.83	−0.24	0.80	0.96
VLUC	22.27	16.39	0.43	0.45	−0.32	2.15	−0.14	0.91	1.06
VVLO	22.81	18.10	0.53	0.57	0.74	3.63	0.95	1.26	2.15
ZIMM	20.26	15.21	0.41	0.42	0.23	−0.02	0.16	0.79	1.36

How epochs of equipment changes are derived is described in this work in the data archiving section.

Because of the existence of abnormal outliers in daily solutions, so that the scatter does not obey Gaussian statistics, the robust-fit algorithm embedded in the QOCA software, which resists outliers better than conventional least squares (Bock *et al.*, 2000), is employed to estimate all the parameters simultaneously.

Table III provides the time-series parameters described above and derived for the central Mediterranean stations that observed for more than 3 years, and in particular the annual and semiannual amplitudes (*c*, *d*, *e* and *f*) terms, referred to January 1*th*, the Weighted Root Mean Squares (WRMS) of the time-series after removal of constant slope (velocity), and the computed offsets values, with 1σ uncertainties, are listed. ITRF2000 horizontal and vertical velocities, with 1σ uncertainties, are listed in table IV. The north, east and up detrended position time-series, with annual and semi-annual signals, for the Italian stations are shown in fig. 5a-d.

4.4. *GPS rate error estimate*

The use of least-squares procedures to compute station velocities from position time-series provides formal uncertainties that are rather unrealistic. The usual assumption that measurement errors are random and uncorrelated from one epoch to the next (white noise) is violated with GPS data (Johnson and Agnew, 1995). The source of time-correlated (colored) noise in GPS data includes orbits, atmospheric effects and monument motions (Langbein and Johnson, 1997; Mao *et al.*, 1999). If colored noise is present, but only pure white noise is assumed, GPS velocity errors can be significantly underestimated (Zhang *et al.*, 1997). Williams *et al.* (2004) studied the position time-series of 414 CGPS

sites, and confirmed previous results, suggesting that white and flicker noise are clearly the dominant noise model, although there are more sites in their solutions where white noise plus random walk noise is the preferred one. The random walk noise component is in any case more difficult to be detected, since it asks for much longer time spans.

The temporally correlated noise that dominates GPS time-series can be adequately described as flicker noise, which is spatially correlated, and has a clear latitude dependence. Although the amplitude of the flicker noise has decreased in time since the first CGPS sites began producing data (early '90), it is still the dominant colored noise process (Williams *et al.*, 2004). The vertical magnitudes are about 3 times larger than the horizontal ones.

In order to compute more realistic rate errors we adopt the approach of Mao *et al.* (1999), who developed an empirical model for estimating the GPS rate error (σ_r) for individual velocity components (north, east and vertical) using position time-series in presence of combined white and colored noise (flicker plus random walk). In our analysis we compute final rate errors using the formula

$$\sigma_r^2 \cong \frac{12\sigma_w^2}{gT^3} + \frac{a\sigma_f^2}{g^bT^2} + \frac{a\sigma_{rw}^2}{gT}$$

where g is the number of measurements per year, T is the total observation time span of observations (listed in table III), a and b are empiric constants, given in Mao *et al.* (1999) ($a = 1.78$; $b = 0.22$). Noise magnitudes for white and flicker components, given in mm, and for the random walk component, given in mm/√yr, have been computed considering the strong linear correlation observed by Mao *et al.* (1999) between the WRMS of GPS time-series and the corresponding white and flicker noise amplitudes. We use the WRMS obtained from the robust fit analysis


Fig. 5a-d. Position time-series (after removing the constant velocity) of the Italian stations that observed for more than 3 years. The red error bars represent 1σ standard deviation formal uncertainties obtained from the GAMIT/GLOBK analysis. Annual and semiannual signals are also displayed, with uncertainties (red curve). Dotted black lines show the epochs of the significant offsets in the time-series that have been computed and corrected (epochs and offsets values are listed in table III).
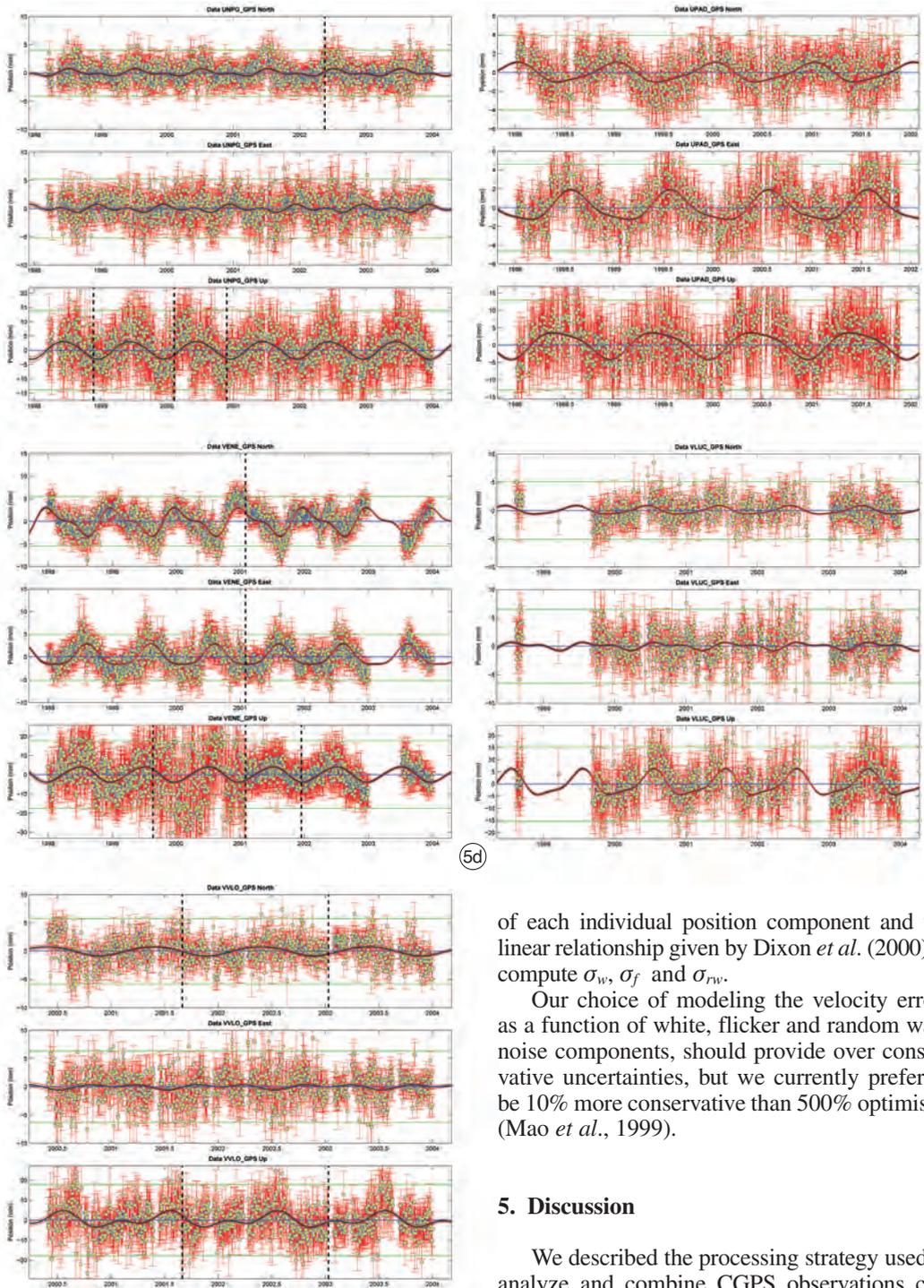
(5a)

(5b)

(5c)
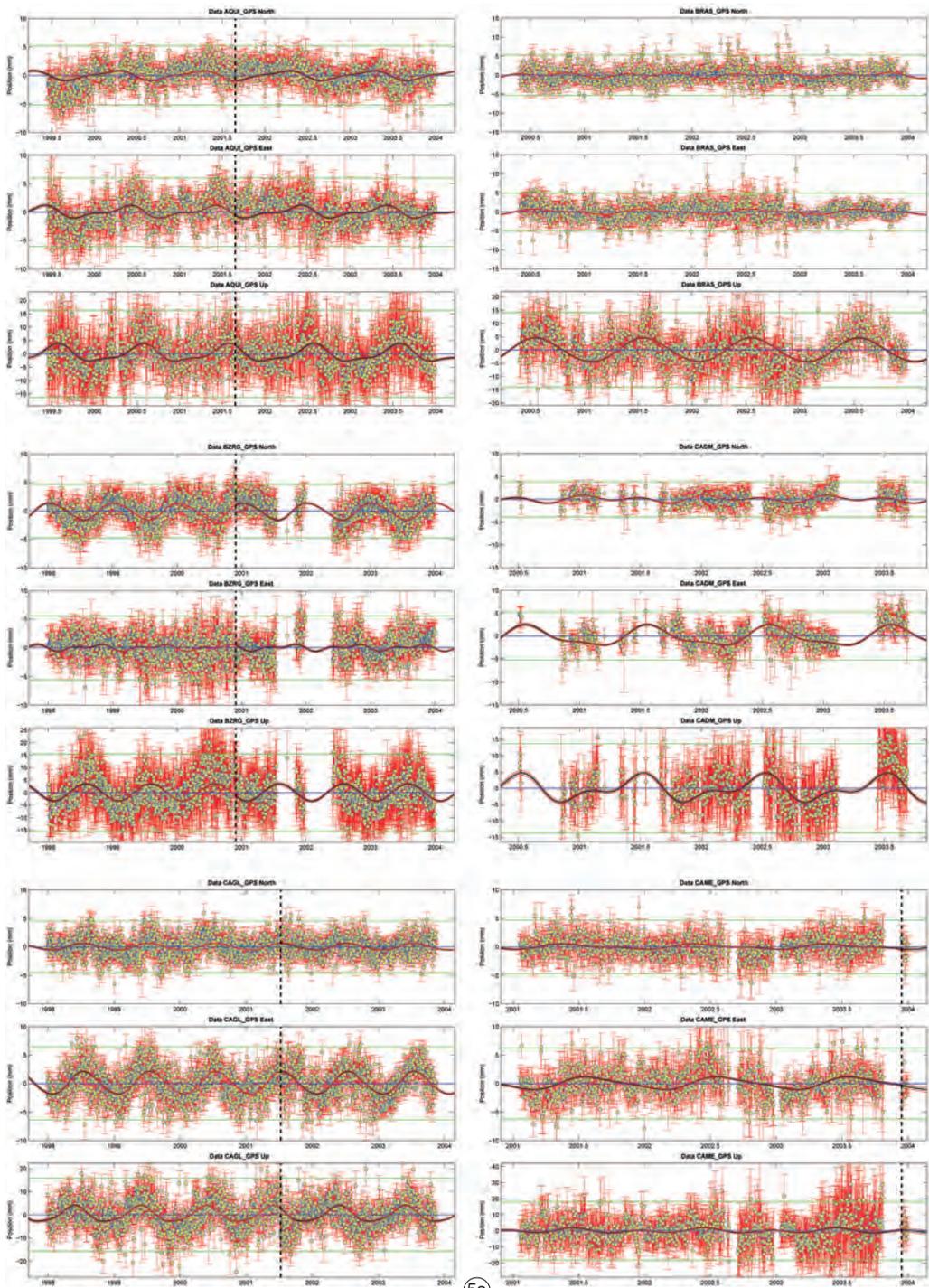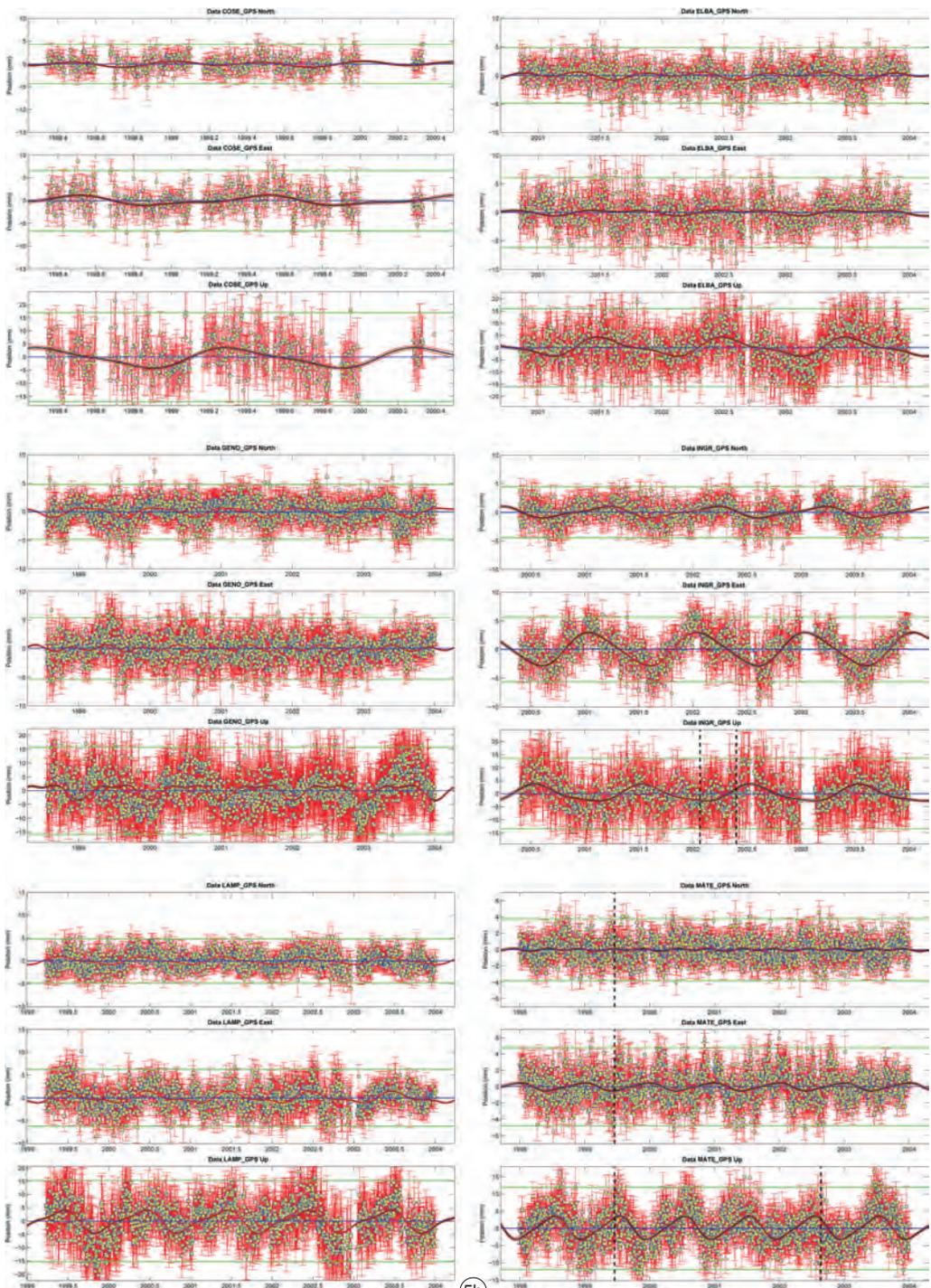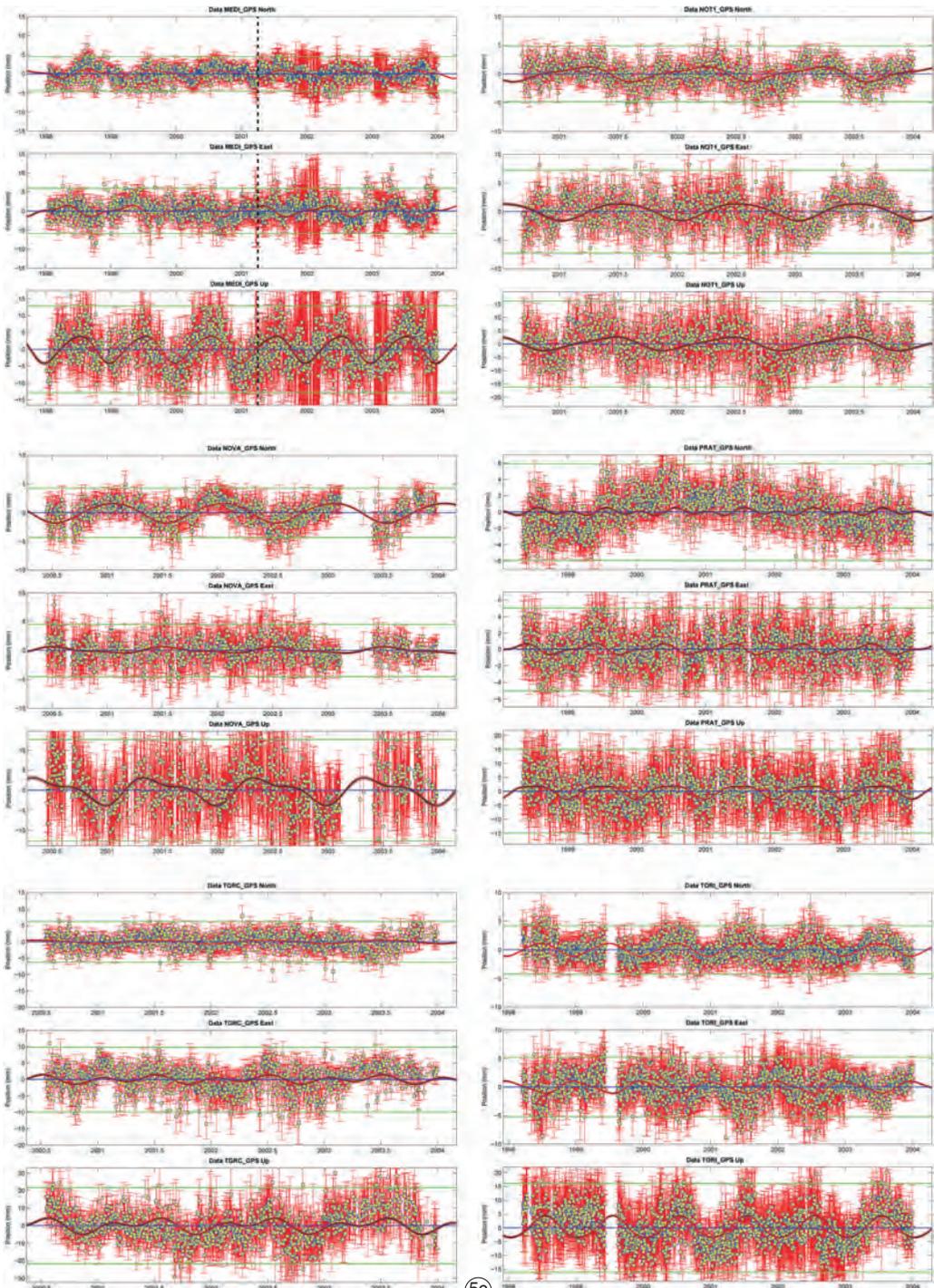
of each individual position component and the linear relationship given by Dixon *et al.* (2000) to compute σ_w, σ_f and σ_{rw}.

Our choice of modeling the velocity errors as a function of white, flicker and random walk noise components, should provide over conservative uncertainties, but we currently prefer to be 10% more conservative than 500% optimistic (Mao *et al.*, 1999).

5. Discussion

We described the processing strategy used to analyze and combine CGPS observations col-

lected at different networks in the Euro-Mediterranean region, with the aim of producing a self-consistent three dimensional velocity field suitable for geodynamics and tectonic applications. Caporali (2003), from the analysis of CGPS stations, found that the rates estimated from position time-series become stable after an observation window of at least three years. For this reason we only discuss results obtained from the analysis of the 31 sites of our data set that observed more than three years (see table III).

The main product of our analysis is, for each station, a set of three dimensional position time-series, provided in a uniform and well defined global frame of reference (the ITRF2000). These time-series are used to compute horizontal and vertical velocities, assumed constant in time, and obtained trough a robust fit algorithm, which is less sensitive to the outliers and blunders present in the raw series, together with annual and semi-annual seasonal signals and epoch offsets. Although seasonal signals are in general quite small (at mm level), some stations display offsets as large as 9 cm (*i.e.*, VENE). It is worth noting that larger offsets are usually observed in the vertical components, and are commonly due to changes in the GPS antenna configuration, as deduced by station log-files.

The mean values of post-fit WRSM for the north, east and vertical components (see table III) are about 1.7 mm, 1.8 mm and 4.8 mm, respectively. The station TGRC, in particular, is the worst site analyzed, displaying values of 2.08 mm, 3.28 mm and 7.24 mm in the three components as above, with a large data scatter, and an unclear seasonal signature (see fig. 5c). In general, a model that considers also the seasonal terms reduces the mean WRMS values by 4%, 3% and 6% for the north, east and vertical components, respectively.

The computed seasonal signals, listed in table III, and displayed in fig. 5a-d only for some of the stations analyzed, are in average significantly below the 1 mm level for the horizontal components, whereas are larger than the 1 mm level in the vertical component.

The mean annual cosine and sine amplitudes for the north components are 0.55 ± 0.06 mm and 0.39 ± 0.06 mm, respectively, with the largest value observed at Venice (VENE: 2.40

mm) and Sarajevo (SRJV: 1.04 mm). The mean annual cosine and sine amplitudes for the east component are 0.66 ± 0.08 mm and 0.39 ± 0.08 mm, respectively, with the largest values observed at Rome (INGR: 2.58 mm) and Venice (VENE: 1.38 mm). The mean annual cosine and sine amplitudes for the vertical component are 2.79 ± 0.20 mm and 1.06 ± 0.21 mm, respectively, with largest values observed at Venice (VENE: 4.83 mm) and Osje (OSJE: 3.41 mm).

As regards the semi-annual terms, the mean cosine and sine amplitudes for the north component are 0.19 ± 0.06 mm and 0.18 ± 0.06 mm, respectively, with the largest values observed at Venice (VENE: 0.59 mm and 0.96 mm). The mean cosine and sine amplitudes for the east component are both 0.23 ± 0.08 mm, with the largest values observed at Reggio Calabria (TGRC: 0.92 mm) and Venice (VENE:0.56 mm). The mean cosine and sine amplitudes for the vertical component are 0.57 ± 0.20 mm and 0.53 ± 0.20 mm, respectively, with the largest values observed at Castel del Monte (CADM: 1.61 mm) and Reggio Calabria (TGRC: 2.40 mm).

In our processing procedures we compute and remove the seasonal terms in order to reduce the daily data scatter and look at residual time-series, with the aim of improving the determination of the constant velocity term, which is the main goal of our analysis. Seasonal signals are generally related to: 1) gravitational excitation, 2) thermal origin coupled with hydrodynamics, 3) sources that are indirect due to geophysical processes, or of instrument, or modeling deficiency (Dong *et al.*, 2002). The first category comprises rotational displacements due to seasonal polar motion (UT1), and loading induced displacement caused by solid Earth, ocean and atmospheric tides, which are modeled in the raw data reduction step (see Section 5.1). However, residual ocean tide effects should still be present, and are mainly due to the use of global ocean tide models instead of higher quality local tidal models. Pole tide loading also belongs to this first category, with the spectrum of mostly annual and Chandler wobble periods (~465 days). The deformation caused by pressure field variation, non-tidal sea surface fluctuation, ground water changes in

both liquid and solid form, bedrock expansion beneath the GPS benchmark, and wind shear belong to the second category. The third category contains other error sources, which also generate apparent seasonal variations, such as orbit modeling errors caused by imperfect reference frame, which is defined through a set of stations that are subject to seasonal variations. There are other important phenomena that can affect the position time-series with a seasonal signature; these involve tectonic-induced deformation, due to possible seasonal variations in regional fault slip or regional stress (*e.g.*, slow earthquakes; Miller *et al.*, 2002), and this is one of the main reasons for which detecting non-tectonic signatures is a fundamental task. Table V provides the magnitudes of some individual sources that can potentially affect the GPS time-series (Dong *et al.*, 2002). Although most of the sources can be modeled and removed from the time-series (*e.g.*, atmospheric mass loading, non-tidal mass loading, snow and soil moisture loading related effects) there is a set of complex sources that are much more difficult to asses and model. These includes: 1) neglected seasonal effects in the definition of the ITRF reference frame; 2) imperfect atmospheric modeling (Williams *et al.*, 1998); 3) bedrock thermal expansion, which may affect the site

Table V. Contributions of geophysical sources and model errors to the observed annual and semiannual variations in site positions.

Source	Range of effects
Pole tide	~4 mm
Ocean tide	~0.1 mm
Atmospheric mass	~4 mm
Non-tidal ocean mass	2-3 mm
Snow mass	3-5 mm
Soil moisture	2-7 mm
Bedrock thermal expansion	~0.5 mm
Errors in orbit, phase center, and troposphere models	No quantitative results yet
Error in network adjustment	~0.7 mm
Differences from different software	~2-3 mm, at some sites 5-7 mm

vertical position at 0.5 mm level (Dong *et al.*, 2002); 4) other environmental factors, including types of domes or monuments (Meertens *et al.*, 1996; Bock *et al.*, 2000; Hatanaka *et al.*, 2001). Time independent antenna phase center model and multipath are also influenced by environmental factors, such as filling level of lakes, frozen/unfrozen of large water bodies, even tree trimming (King *et al.*, 1995).

At different sites and networks different noise sources may dominate, and includes residual common mode positioning noise (white plus flicker noise), monument instabilities (random walk noise), and localized deformation due, for example, to changes in groundwater, or other non tectonic local loading. The spatially correlated common mode error (Wdowinsky *et al.*, 1997), is removed, or at least significantly reduced, by performing the 7 parameters Helmert transformation, with regional stations included, and by removing annual and semi-annual signatures; this reduces by a factor of 2-3 the amplitudes of both white and flicker noise components, supporting Williams *et al.* (2004) explanation that a significant amount of the flicker noise is due to a common physical basis, with large spatial extend. The remaining flicker noise is probably due to regional-scale processes such as atmospheric effects, and not to monument motions. Geodetic monument instability due to varying conditions of the anchoring media (*e.g.*, soil, bedrock, building) is considered an important source of noise, thought to follow a random walk process (Johnson and Agnew, 1995; Langbein and Johnson, 1997). Whether or not the random walk noise is detectable depends on the length of the time-series, the sampling frequency, and the relative amplitudes of the other noise components. Random walk noise has been identified in continuous strain-meter data (Wyatt, 1982; Wyatt *et al.*, 1989), and can be as high as 3 mm/√yr for some geodetic data (Johnson and Agnew, 1995). However, this type of disturbance can be mitigated by carefully designed monuments. The use of deeply anchored Wyatt design monuments (Wyatt *et al.*, 1989; Bock *et al.*, 1997), for example, provide an amplitude of only 0.4 mm/√yr (Johnson and Agnew, 2000). However, regional GPS networks

have much longer inter-station spacing so that other sources of error, such as known random atmospheric propagation effects (Williams *et al.*, 1998) could dominate the budget.

The network we analyze is realized through stations characterized by several different monument types (described in table I). Pillars, or steel musts, anchored to stable buildings represent the largest number, while monuments directly founded on more and less consolidated bedrock are of different types: mainly concrete pillars, with some mast (*i.e.*, VVLO) and tripod (*i.e.*, TRO1). Since potential monument noise should be related to the stability of the monument itself with respect to potential local processes (*i.e.*, soil

humidity content and water table level changes, bedrock thermal expansion, etc), its constructive quality depends on how much the monument is able to reduce its response to those effects. However, we do not find any significant correlation between seasonal term amplitudes and monument types. Stations realized through pillars founded directly on bedrock (*e.g.*, AJAC, AQUI, CAGL, CAME, ELBA, GRAS, NOT1, ORID, VVLO) perform very well, with relatively lower amplitudes on both horizontal and vertical components. It is worth noting that also stations built on buildings (*e.g.*, BRAS, GENO, GRAZ, MATE, PRAT, UNPG) perform quite well, displaying horizontal seasonal amplitudes signifi-
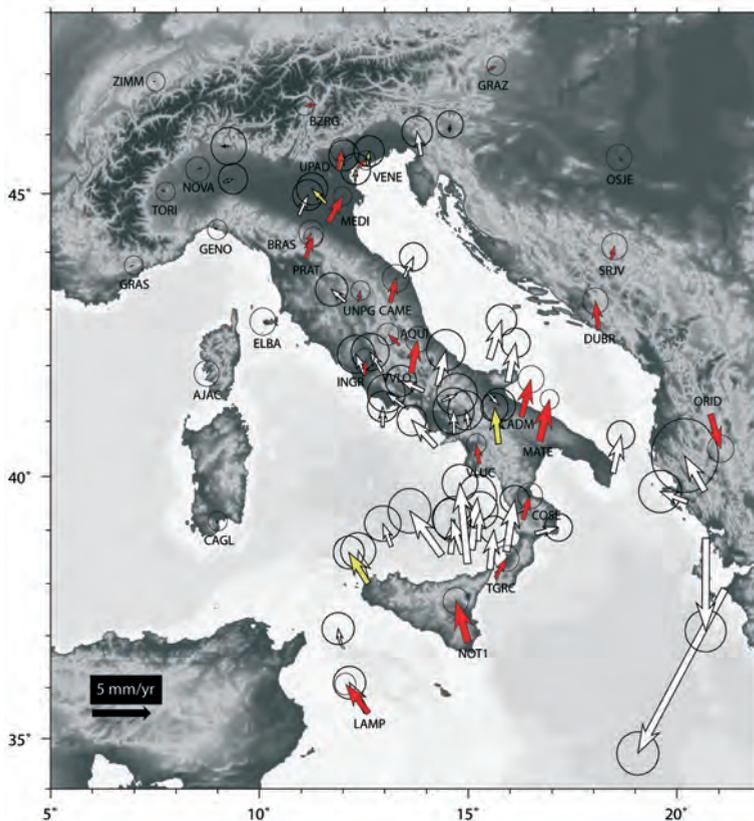
Fig. 6a. Residual velocities (in mm/yr), and 95% error ellipses, given with respect to the stable Eurasian frame described in Serpelloni *et al.* (2005). Red arrows: velocities of CGPS stations that observed for more than three years; yellow arrows: velocities for CGPS stations that observed for less than three years; white arrows: velocities from non-permanent stations surveyed in the 1991-2004 time span (Serpelloni *et al.*, 2005).

Fig. 6b. Residual vertical velocities (in mm/yr), with one standard deviation error bars, given with respect to the stable Corsica-Sardinia block. Numbers are given only for stations showing significant vertical rates.

cantly below the 1 mm level. Only very bad monuments, like the one used for the station VENE, display very large amplitudes on both horizontal and vertical seasonal components. These observations, even if preliminary, are in agreement with results given by Williams *et al.* (2004), who analyzed noise characteristics of regional network solutions (in particular from the SCIGN network in Southern California) to put some constraints on the quality of the different CGPS monuments involved. Williams *et al.* (2004) analysis reveals that they found that deeply anchored Wyatt-designed monuments perform better that all other types, but also stations mounted on stable buildings are quite good.

To map our velocity solution into a reference frame that can be used for geo-kinematics interpretations of the study area, the horizontal ITRF velocities are rotated into a fixed Eurasian frame, and the vertical velocities are given with respect to an external stable frame (*i.e.*, Sardinia-Corsica block or Central Europe). Figure 6a displays the residual velocities given with respect to the Eurasian fixed frame proposed by Serpelloni *et al.* (2005) of CGPS stations that observed for more than three years, together with velocities of CGPS stations that observed less than three years and non-permanent stations from Serpelloni *et al.* (2005). Vertical velocities are instead proposed with respect to a regionally stable external frame. In this work we used as stable area the Corsica-Sardinia region, which has been observed to be stable with respect to Eurasia both in terms of horizontal

and vertical motions. Figure 6b displays the vertical rates, with one standard deviation errors, of CGPS stations that observed for more than three years.

6. Conclusions

We described the procedures routinely used to download, store and analyze data from continuous GPS networks operating in the Mediterranean and European region, with the goal of deriving a self-consistent three dimensional velocity field that can be used for further geodynamics and geo-kinematics applications. The method used is based on a «distributed session» approach and provides several advantages, that can be summarized as following: 1) it makes an efficient use of computing resources; 2) it allows for the determination of a self-consistent set of station velocities in a uniform reference frame; 3) it allows for a rigorous combination among different space geodetic solutions; 4) it allows for a combination of continuous and campaign GPS observations into the same reference frame.

We performed an analysis of the position time-series for all the stations that observed for more than three years, with the aim of providing station velocities, together with the amplitudes of the annual and semi-annual signals and the offsets observed in the series. The final result of our analysis is presented in terms of tables, reporting the velocity values and the amplitudes of the detected signals, and in terms of maps of horizontal and vertical velocities, given with respect to uniformly defined external stable frames.

Recent papers dealing with GPS observations in Italy and its surroundings revealed scientific problems about the kinematics and geodynamics of this region that will certainly benefit from the enlargement and improvement of the CGPS network, but that also require a multidisciplinary approach through the integration of seismological, geological and other geophysical and geodetic data (*e.g.*, non-permanent networks, leveling measurements). In particular, the kinematics of Sicily with respect to Nubia (Africa), and its possible microplate-like behavior, is still matter of debate (Hollenstein *et al.*,

2003; D'Agostino and Selvaggi, 2004; Serpelloni *et al.*, 2005). In northeastern Sicily and Central Aeolian region large deformation rates and «anomalously» high horizontal velocities have been observed at non-permanent GPS stations (Hollenstein *et al.*, 2003; Serpelloni *et al.*, 2005), and earthquake focal solutions reveal a rapid change in the seismotectonic setting east and west of the Salina-Lipari-Vulcano lineament (Pondrelli *et al.*, 2004). Open questions for this area, which interests also the Messina Straits, involve the role of the Calabrian slab and the kinematics of the Ionian and Calabrian blocks, in the frame of a complex plate-boundary configuration (Goes *et al.*, 2004). While upper bounds of active extension across the Apennines have been recently proposed (*e.g.*, Hunstad *et al.*, 2003; Serpelloni *et al.*, 2005), detailed information on how this deformation is distributed or localized across the active fault zones are still missing for most of the chain, and only dense non-permanent GPS networks are providing preliminary results (Anzidei *et al.*, 2005). GPS data revealed the motion of the Adriatic block as independent, or partially independent, from the African plate (Battaglia *et al.*, 2004). However, Adria internal deformation and boundaries with respect to the African and Ionian domains are still unclear. At the same time, the possible presence of two partially independent Adriatic blocks is still matter of debate (Oldow *et al.*, 2002; Battaglia *et al.*, 2004; D'Agostino *et al.*, 2005; Serpelloni *et al.*, 2005). The Northern Apennines and Po Plain region are still poorly understood from a kinematic point of view, also due to the low deformation rates involved (Serpelloni *et al.*, 2005), and the main goal of geodetic research in this region is to study where active extensional and compressional strains are localized across the belt, toward the Po Plain and the Adriatic (http://earth.geology.yale.edu/RETREAT/).

The distributed processing mode adopted in this work allows us to look at the data collected at regional or local scale GPS networks, both permanent and non-permanent, from a global point of view, that is to include local or regional deformations (related for example to single fault segments) in a «plate tectonic» framework, with large advantages for a better comprehension of

the tectonic and geodynamics processes that are deforming the crust in the Italian region.

Acknowledgements

REFERENCES

ABRAMOWITZ, M. and I.A. STEGUN (Editors) (1972): *Handbook of Mathematical Functions with Formulas, Graphs, and Mathematical Tables* (Dover, New York), 9th printing.

ALTAMIMI, Z., P. SILLARD and C. BOUCHER (2002): ITRF2000: a new release of the International Terrestrial Reference Frame for earth science applications, *J. Geophys. Res.*, **107** (B10), 2214, doi: 10.1029/ 2001JB000561.

ANZIDEI, M., P. BALDI, C. BONINI, G. CASULA, S. GANDOLFI and F. RIGUZZI (1998): Geodetic surveys across the Messina Straits (Southern Italy) seismogenic area, *J. Geodyn.*, **25** (2), 85-97.

ANZIDEI, M., P. BALDI, A. PESCI, A. ESPOSITO, A. GALVANI, F. LODDO, P. CRISTOFOLETTI, A. MASSUCCI and S. DEL MESE (2005): Geodetic deformation across the Central Apennines from GPS data in the time Span 1999-2003, *Ann. Geophysics*, **48** (2), 259-271.

BATTAGLIA, M., M. MURRAY, E. SERPELLONI and R. BURGMANN (2004): The Adriatic region: an independent microplate within the Africa-Eurasia collision zone, *Geophys. Res. Lett.*, **31**, L09605, doi: 10.1029/ 2004GL019723.

BLEWITT, G., Y. BOCK and G. GENDT (1993): Regional clusters and distributed processing, in *Proceedings of the IGS Analysis Center Workshop*, Ottawa, Canada, 62-91.

BOCK, Y., S.A. GOUREVITCH, C.C. COUNSELMAN III, R.W. KING and R.I. ABBOT (1986): Interferometric analysis of GPS phase observations, *Manuscripta Geodetica*, **11**, 282-288.

BOCK, Y., S. WDOWINSKI, P. FANG, J. ZHANG, S. WILLIAMS, H. JOHNSON, J. BEHR, J. GENRICH, J. DEAN, M. VAN DOMSELAAR, D. AGNEW, F. WYATT, K. STARK, B. ORAL, K. HUDNUT, R.W. KING, T.H. HERRING, S. DINARDO, W. YOUNG, D. JACKSON and W. GURTNER (1997): Southern California permanent GPS geodetic array: continuous measurements of regional crustal deformation between the 1992 Landers and 1994 Northridge earthquakes, *J. Geophys. Res.*, **102** (B8), 18013-18034, doi: 10.1029/ 97JB01379.

BOCK, Y., R.M. NIKOLAIDIS, P.J. DE JONGE and M. BEVIS (2000): Instantaneous geodetic positioning at medium distances with the Global Positioning System, *J. Geophys. Res.*, **105** (B12), 28223-28254, doi: 10.1029/ 2000JB000268.

CALAIS, E., R. BAYER, J. CHÉRY, F. COTTON, M. FLOUZAT, F. JOUANNE, J. MARTINOD, F. MATHIEU, O. SCOTTI, M. TARDY and C. VIGNY (2000): REGAL: A permanent GPS network in the French Western Alps, Configuration and first results, *C.R. Acad. Sci. Paris*, **331**, 435-442.

CAPORALI, A. (2003): Average strain rate in the Italian crust inferred from a permanent GPS network, I. Statistical analysis of the time-series of permanent stations, *Geophys. J. Int.*, **155**, 241-253.

D'AGOSTINO, N. and G. SELVAGGI (2004): Crustal motion along the Eurasia-Nubia plate-boundary in the Calabrian Arc and Sicily and active extension in the Messina Straits from GPS measurements, *J. Geophys. Res.*, **109** (B11), 402, doi: 10.1029/2004JB002998.

D'AGOSTINO, N., D. CHELONI, S. MANTENUTO, G. SELVAGGI, A. MICHELINI and D. ZULIANI (2005): Strain accumulation in the Southern Alps (NE Italy) and deformation at the northeastern boundary of Adria observed by CGPS measurements, *Geophys. Res. Lett.*, **32**, L19306, doi: 10.1029/2005GL024266.

DING, X.L., D.W. ZHENG, D.N. DONG, C. MA, Y.Q. CHEN and G.L. WANG (2005): Seasonal and secular positional variations at eight co-located GPS and VLBI stations, *J. Geod.*, **79** (1-3), 71-81.

DIXON, T.H., M. MILLER, F. FARINA, H. WANG and D. JOHNSON (2000): Present-day motion of the Sierra Nevada block and some tectonic implications for the basin and Range province, North American Cordillera, *Tectonics*, **19** (1), 1-24.

DONG, D. and Y. BOCK (1989): Global Positioning System network analysis with phase ambiguity resolution applied to crustal deformation studies in California, *J. Geophys. Res.*, **94**, 3949-3966.

DONG, D., T.A. HERRING and R.W. KING (1998): Estimating regional deformation from a combination of space and terrestrial geodetic data, *J. Geod.*, **72**, 200-214.

DONG, D., P. FANG, Y. BOCK, M.K. CHENG and S. MIYAZAKI (2002): Anatomy of apparent seasonal variation from GPS-derived site position, *J. Geophys. Res.*, **107**, doi: 10.1029/2001JB000573.

GOES, S., D. GIARDINI, S. JENNY, C. HOLLENSTEIN, H.G. KHALE and A. GEIGER (2004): A recent tectonic reor-

ganization in the south-central Mediterranean, *Earth Planet. Sci. Lett.*, **226**, 335-345.

HATANAKA, Y., M. SAWADA, A. HORITA, M. KUSAKA, J. JOHNSON and C. ROCKEN (2001): Calibration of antenna-radome and monument-multipath effect on GEONET, Part 2. Evaluation of the phase map by GEONET data, *Earth Planets Space*, **53**, 23-30.

HEFLIN, M., W. BERTIGER, G. BLEWITT, A. FREEDMAN, K. HURST, S. LICHTEN, U. LINDQUISTER, Y. VIGUE, F. WEBB, T. YUNCK and J. ZUMBERGE (1992): Global geodesy using GPS without fiducial sites, *Geophys. Res. Lett.*, **19**, 131-134.

HERRING, T.A. (2000): *GLOBK: Global Kalman Filter VLBI and GPS Analysis Program Version 10.0* (Massachusetts Institute of Technology, Cambridge).

HERRING, T.H., J.L. DAVIS and I.I. SHAPIRO (1990): Geodesy by radio interferometry: the application of Kalman filtering to the analysis of very long baseline interferometry data, *J. Geophys. Res.*, **95** (B8), 12561-12581, doi: 10.1029/90JB00683.

HERRING, T.H., D. DONG and R.W. KING (1991): Sub-milliarcsecond determination of pole position using the Global Positioning System, *Geophys. Res. Lett.*, **18**, 1893-1896.

HOLLENSTEIN, CH., H.G. KAHLE, A. GEIGER, S. JENNY, S. GOES and D. GIARDINI (2003): New GPS constraints on the Africa-Eurasia plate-boundary zone in Southern Italy, *Geophys. Res. Lett.*, **30** (18), 1935, doi: 10.1029/2003GL017554.

HUNSTAD, I., G. SELVAGGI, N. D'AGOSTINO, P. ENGLAND, P. CLARKE and M. PIEROZZI (2003): Geodetic strain in peninsular Italy between 1875 and 2001, *Geophys. Res. Lett.*, **30** (4), 1181, doi: 10.1029/2002GL016447.

JOHNSON, H. and D. AGNEW (1995): Monument motion and measurements of crustal velocities, *Geophys. Res. Lett.*, **22**, 2905-2908.

JOHNSON, H. and D. AGNEW (2000): Correlated noise in geodetic time series, *U.S. Geol. Surv., Final tech. Rep., FTR-1434-HQ-97-GR-03155*.

KING, R.W. and Y. BOCK (2000): *Documentation for GAMIT GPS Analysis Software, Version 10.01* (Massachusetts Institute of Technology and Scripps Institution of Oceanography).

KING, N.E., J.L. SVARC, E.B. FOGLEMAN, W.K. GROSS, K.W. CLARK, G.D. HAMILTON, C.H. STIFFLER and J.M. SUTTON (1995): Continuous GPS observations across the Hayward Fault, California, 1991-1994, *J. Geophys. Res.*, **100** (B10), 20271-20284, doi: 10.1029/95JB02035.

KING, R.W., J. COLLINS, E.M. MASTERS, C. RIZOS and A. STOLZ (1985): Surveying with Global Positioning System (School of Surveying, University of New South Wales, Sydney), *Monograph No. 9*.

LANGBEIN, J. and H. JOHNSON (1997): Correlated errors in geodetic time series: implications for time-dependent deformation, *J. Geophys. Res.*, **102**, 591-603.

LARSON, K.M., J.T. FREYMUELLER and S. PHILIPSEN (1997): Global plate velocities from the Global Positioning System, *J. Geophys. Res.*, **102**, 591-603.

MAO, A., C.G.A. HARRISON and T.H. DIXON (1999): Noise in GPS coordinate time series, *J. Geophys. Res.*, **104**, 2797-2816.

MCCARTHY, D.D. (Editor) (1996): IERS Conventions 1996 (Int. Earth Rotations Serv., Obs. de Paris), *IERS Tech. Note 21*.

MCCLUSKY, S., R. REILINGER, S. MAHMOUD, D. BEN SARI and A. TEALEB (2003): GPS constraints on Africa (Nubia) and Arabia plate motions, *Geophys. J. Int.*, **155**, 126-138.

MEERTENS, C., C. ALBER, J. BRAUN, C. ROCKEN, B. STEPHENS, R. WARE, M. EXNER and P. KOLESNIKOFF (1996): Field and anechoic chamber tests of GPS antennas, in *Proceedings of IGS Analysis Center Workshop*, June 1996, Silver Springs, MD, U.S.A., 107-118.

MILLER, M.M., T. MELBOURNE, D.J. JOHNSON and W.Q. SUMNER (2002): Periodic slow earthquakes from the Cascadia subduction zone, *Science*, **295** (5564), 2423.

NOCQUET, J.M. and E. CALAIS (2003): Crustal velocity field of Western Europe from permanent GPS array solutions, 1996-2001, *Geophys. J. Int.*, **154**, 72-88.

OLDOW, J.S., L. FERRANTI, D.S. LEWIS, J.K. CAMPBELL, B. D'ARGENIO, R. CATALANO, G. PAPPONE, L. CARMIGNANI, P. CONTI and C.L.V. AIKEN (2002): Active fragmentation of Adria, the North African promontory, Central Mediterranean orogen, *Geology*, **30** (9), 779-782.

PONDRELLI, S., C. PIROMALLO and E. SERPELLONI (2004): Convergence *versus* retreat in Southern Tyrrhenian Sea: insights from kinematics, *Geophys. Res. Lett.*, **31**, L0661, doi: 10.1029/2003GL019223.

SANSÒ, F. and M.C. DE LACY (2000): *Uno Studio sulle Diverse Applicazioni del GPS e sul Futuro Sviluppo della Rete di Stazioni Permanenti GPS sul Territorio Italiano Orientato alla Creazione di un Servizio Geodetico Nazionale* (available on line at http://geomatica.como.polimi.it/gps/articoli/asi.pdf).

SCHAFFRIN, B. and Y. BOCK (1988): A unified scheme for processing GPS dual-band phase observations, *Bull. Géod.*, **62**, 142-160.

SCHERNECK, H.G. (1991): A parameterized solid Earth tide model and ocean tide loading effects for global geodetic baseline measurements, *Geophys. J. Int.*, **106**, 677-694.

SERPELLONI, E., M. ANZIDEI, P. BALDI, G. CASULA, A. GALVANI, A. PESCI and F. RIGUZZI (2002): Combination of permanent and non-permanent GPS networks for the evaluation of the strain-rate field in the central Mediterranean area, *Boll. Geofis. Teor. Appl.*, **43,** 195-219.

SERPELLONI, E., M. ANZIDEI, P. BALDI, G. CASULA and A. GALVANI (2005): Crustal velocity and strain-rate fields in Italy and surrounding regions: new results from the analysis of permanent and non-permanent GPS networks, *Geophy. J. Int.*, **161** (3), 861-880, doi: 10.1111/j.1365-246X.2005.02618.x.

WDOWINSKI, S., Y. BOCK, J. ZHANG, P. FANG and J. GENRICH (1997): Southern California permanent GPS geodetic array: spatial filtering of daily positions for estimating coseismic and postseismic displacements induced by the 1992 Landers earthquake, *J. Geophys. Res.*, **102** (B8), 18057-18070, doi: 10.1029/97JB01378.

WESSEL, P. and W.H.F. SMITH (1995): New Version of the generic mapping tools released, *Eos, Trans. Am. Geophys. Un.*, **76**, 329.

WILLIAMS, S., Y. BOCK and P. FANG (1998): Integrated satellite interferometry: tropospheric noise, GPS estimates and implications for interferometric synthetic aperture radar products, *J. Geophys. Res.*, **103** (B11), 27051-27068, doi: 10.1029/98JB02794.

WILLIAMS, S.D.P., Y. BOCK, P. FANG, P. JAMASON, R.M. NIKOLAIDIS, L. PRAWIRODIRDJO, M. MILLER and D.J. JOHNSON (2004): Error analysis of continuous GPS po-

sition time series, *J. Geophys. Res.*, **109**, B03412, doi: 10.1029/2003JB002741.

WYATT, F.K. (1982): Displacement of surface monuments: horizontal motion, *J. Geophys. Res.*, **87**, 979-989.

WYATT, F.K., H. BOLTON, S. BRALLA and D. AGNEW (1989): New designs of geodetic monuments for use with GPS, *Eos, Trans. Am. Geophys. Un.*, **70**, 1054.

ZHANG, J., Y. BOCK, H. JOHNSON, P. FANG, S. WILLIAMS, J. GENRICH, S. WDOWINSKI and J. BEHR (1997): Southern California permanent GPS geodetic array: error analysis of daily position estimates and site velocities, *J. Geophys. Res.*, **102**, 18.035-18.055.